IEEE Access
Multidisciplinary | Rapid Review | Open Access Journal

Received December 22, 2019, accepted January 15, 2020, date of publication January 21, 2020, date of current version January 30, 2020.

Digital Object Identifier 10.1109/ACCESS.2020.2968476

IWORMLF: Improved Invasive Weed Optimization With Random Mutation and Lévy Flight for Beam Pattern Optimizations of Linear and Circular Antenna Arrays

TINGTING ZHENG[1], YANHENG LIU[1,2], GENG SUN[1,2,3], (Member, IEEE), LIN ZHANG[4], SHUANG LIANG[1], AIMIN WANG[1,2], AND XU ZHOU[2]

[1]College of Computer Science and Technology, Jilin University, Changchun 130012, China
[2]Key Laboratory of Symbolic Computation and Knowledge Engineering of Ministry of Education, Jilin University, Changchun 130012, China
[3]College of Communication Engineering, Jilin University, Changchun 130012, China
[4]Financial Department, Jilin University, Changchun 130012, China

Corresponding author: Geng Sun (sungeng@jlu.edu.cn)

This work was supported in part by the National Natural Science Foundation of China under Grant 61872158, in part by the National Science Foundation for Young Scientists of China under Grant 61806083, in part by the Postdoctoral Innovative Talent Support Program of China under Grant BX2018128, in part by the China Postdoctoral Science Foundation under Grant 2018M640283, in part by the Science and Technology Development Plan Project of Jilin Province under Grant 20190701019GH, and in part by the China Guanghua Science and Technology Foundation of the First Hospital of Jilin University under Grant JDYYGH2019031.

ABSTRACT The beam pattern synthesis of antenna arrays is one of the most significant optimization problems in the electromagnetics community, and it affects the performance of wireless communication systems. In this article, we formulate the beam pattern optimization problems, and propose an improved invasive weed optimization with random mutation and Lévy flight (IWORMLF) algorithm to synthesize the beam patterns of linear antenna arrays (LAAs) and circular antenna arrays (CAAs). IWORMLF introduces the random mutation operator and the Lévy flight mechanism to enhance the efficiency and to balance the exploration and exploitation of the algorithm for optimization problems. Several simulations are conducted to evaluate the performance of the proposed approach. First, IWORMLF is tested by a variety of benchmark functions, and the results indicate that it achieves the best performance in most of the functions compared to some other algorithms. Second, IWORMLF is utilized for the maximum sidelobe level (SLL) reduction and the joint maximum SLL and mainlobe beamwidth reductions. The results show that it achieves better performances in terms of the convergence rate, stability, and accuracy compared to some evolutionary algorithms for these optimization cases. Third, the efficiencies of the improved factors are verified. Finally, electromagnetism simulations are conducted to evaluate the performance of IWORMLF for the beam pattern optimizations with considering mutual coupling.

INDEX TERMS Antenna array, beam pattern, sidelobe level, invasive weed optimization.

I. INTRODUCTION

The capacity of communication systems is reduced by bottlenecks, which has been exacerbated by the rapid development of both wireless communication technologies and the number of users [1]. Antenna arrays are widely used in wireless, radar, and mobile communication systems [2], because they increase the spectral efficiency and capacity [3], [4]. The properties of an antenna array include the beam pattern, which is important [5] because a beam pattern that contains a strongly directional mainlobe with a low sidelobe level (SLL) will effectively improve the communication quality and reduce interference [6], [7].

In conventional antenna arrays, beam pattern synthesis and SLL reduction problems are classical non-linear optimization problems, and they have been proven to be NP-hard [8]. However, antenna arrays with multiple elements have been gradually applied in many applications, such as

The associate editor coordinating the review of this manuscript and approving it for publication was Kuang Zhang.

fifth generation (5G) communication and satellite communication systems. Therefore, for modern wireless communication applications, it is important to determine how to effectively suppress the maximum SLL of beam patterns of antenna arrays [9], [10].

There are several nature-inspired methods, including evolutionary algorithms and swarm intelligence optimization algorithms, which are suitable for solving beam pattern optimization problems [11]. For example, the genetic algorithm (GA) [12], particle-swarm optimization (PSO) [13], ant colony optimization (ACO) [14], differential evolution (DE) [15], wind-driven optimization (WDO) [16], and the firefly algorithm (FA) [17] have been proposed and widely implemented in many fields, including antenna array beam pattern optimization problems. However, one algorithm is not able to solve all optimization problems effectively. Thus, it is essential to employ an effective and efficient approach to optimize the beam pattern of antenna arrays.

The main contributions of this paper are summarized as follows:

(1) We formulate the maximum SLL reduction optimization problems of linear antenna arrays (LAAs) and circular antenna arrays (CAAs) to optimize beam patterns.

(2) To solve the formulated optimization problem preferably, an invasive weed optimization with random mutation and Lévy flight (IWORMLF) algorithm based on the conventional invasive weed optimization (IWO) is proposed. IWORMLF introduces the random mutation operator and the Lévy flight mechanism to enhance the efficiency and to balance the exploration and exploitation of the algorithm, making it more suitable for beam pattern optimization problems.

(3) The performance of the proposed approach is verified by performing simulations. Several recent algorithms and some classical evolutionary algorithms are introduced for comparison, to evaluate the performance of the proposed IWORMLF in optimizing the beam patterns of antenna arrays. Moreover, the stability of the proposed algorithm is tested.

The rest of this paper is organized as follows. Section 2 presents the related work. Section 3 gives the geometries and array factors of the LAA and CAA. Section 4 formulates the sidelobe suppression optimization problem and joint maximum SLL and mainlobe beamwidth reduction problem. Section 5 proposes the IWORMLF algorithm. Section 6 shows the simulation consequence. Section 7 discusses the boundary handling technology. Finally, Section 8 presents a summary of findings and conclusions.

II. RELATED WORK

Several classical and conventional antenna array SLL reduction methods have been considered to address problems involving antenna array beam pattern optimization. Saputra et al. [18] used the Dolph-Chebyshev power distribution to suppress the SLLs of antenna arrays. Tsunoda et al. [19] proposed a thinning method for suppressing the sidelobe of planar antenna arrays, which is a multistage decision procedure. Xing et al. [20] used the substrate integrated coaxial line feeding technique to reduce both the backlobe level and the SLL of a Q-band patch antenna array simultaneously. The use of conventional methods to optimize an antenna array is complex because there are complicated boundary conditions and interactions of parameters. However, swarm intelligence optimization methods can be applied in almost any application without any restrictions of the optimization problem [8]. Several meta-heuristics have been employed to determine the optimal design of antenna arrays. For example, Tian et al. [21] used GAs to adjust the currents and positions of elements in order to reduce the SLLs. Sharaqa et al. [17] adopted the FA to optimize the SLLs of the CAA and concentric circular antenna array (CCAA). The biogeography-based optimization (BBO) method is used to obtain maximum SLL reduction and nulls control of isotropic LAAs [22]. Moreover, the flower pollination algorithm (FPA) is utilized to design the LAA to achieve maximum SLL reduction [23]. Prerna et al. [24] used the grey wolf optimization (GWO) algorithm to achieve an array pattern with a minimum SLL along with the null placement in specified directions. Pappula et al. [25] adopted the cat swarm optimization (CSO) technique to select the optimal positions of an antenna element in order to achieve SLL suppression, and achieved nulls in several desired directions. The artificial bee colony (ABC) algorithm was applied to reduce the maximum SLL of the uniformly excited LAAs [26]. The ant lion optimization (ALO) algorithm was applied to obtain a beam pattern with the optimized SLL as well as the deep null [27]. Boldini et al. [28] propose to use the social network optimization (SNO) algorithm in planar antenna arrays, and compared the consequence with some other approaches. Khodier et al. [29] also utilized the PSO algorithm to minimize the SLL and control the nulls. However, the stability of PSO for beam pattern synthesis is not mentioned. Singh et al. [30] used the binary spider monkey optimization (binSMO) algorithm to achieve maximum SLL reduction; the cost and size of the antenna array and the results of the algorithm are better than those of existing evolutionary algorithms from the perspective of the convergence rate. Sun et al. [31] employed conventional invasive weed optimization (IWO) [32] to reduce the maximum SLL in the LAA and CAA. Foudazi and Mallahzadeh [33] used conventinoal IWO method for the pattern synthesis of multi-feed reflector antennas and the experimental results show that the algorithm achieves good convergence performance. However, the efficiency of IWO algorithm is not mentioned. Pal et al. [32] adopted IWO to optimize the spacing between the elements of LAA for SLL suppression and null placement control, and they achieve better performance than other comparison approaches, the stability of IWO for these optimization cases is not tested. Although evolutionary algorithms are valid for beam patterns with minimum SLLs,

they suffer from the problem of a slow convergence rate in practical conditions [34].

There are several improved methods (based on recent evolutionary algorithms) that overcome the problems of the original algorithm for many applications. Tubishat et al. [35] proposed an improved whale optimization algorithm (IWOA) for feature selection in Arabic sentiment analysis. In their work, two improvement factors were added to the initialization and end phases of the original whale optimization algorithm (WOA), which can overcome the solutions falling into local optima. The experiment results show that the proposed algorithm achieves a better performance than other algorithms in terms of accuracy and the number of selected features. Adeli et al. [36] developed an adaptive inertia weight-based particle swarm optimization (APSO) technique based on feature selection for image steganalysis. It was proven that the proposed approach achieve better results compared to other similar methods in terms of diversity measure, running time, and stego-image. Wang et al. [37] proposed an improved differential harmony search (IDHS) method for numerical function optimization problems. The proposed IDHS balances the exploitation and exploration searching for the best solution using mutation strategies from the differential evolution (DE). The experimental results show that IDHS increases the convergence speed and enhances the efficiency and effectiveness compared to the original algorithm and other swarm intelligence algorithms. Gao et al. [38] proposed an improved flower pollination algorithm (IFPA) for visual tracking. The experiment results prove the superiority of the proposed IFPA-based tracker compared to three other trackers. Sayed et al. [39] used a new chaotic dragonfly algorithm (CDA) to solve the problem of feature selection. The authors applied chaotic maps in the searching iterations to adjust the parameters of the dragonflies' movements, and this strategy improves the convergence rate and enhances the efficiency compared to the original algorithm. These improved evolutionary algorithms can overcome the shortcomings of the original algorithms, and can effectively improve the algorithm performance when applied in some fields.

In addition, several improved approaches based on swarm intelligence algorithms have been gradually adopted in the design of antenna arrays. Liang et al. [1] proposed an optimization algorithm called cuckoo search-chicken swarm optimization (CSCSO) to achieve the maximum SLL reduction of the antenna arrays. Although the proposed CSCSO achieves better results in terms of the convergence rates, the stability of this algorithm has not been tested. Li et al. [6] developed a BBO based on the local search (BBOLS) algorithm to suppress the SLLs of LAAs and CAAs, and the effectiveness of the algorithm was evaluated. However, in their work, the number of elements was 32, which may be not large enough to verify the performance of the proposed approach. Singh et al. [40] proposed an improved FA approach called enhanced firefly algorithm (EFA). This algorithm is applied to the synthesis of the LAA, and the results indicate that EFA provides a faster convergence rate compared to some meta-heuristics methods and the Taguchi method. Sun et al. [41] proposed a SLL reduction method based on the hierarchical cuckoo search (HCS) algorithm, and the authors report that this algorithm is suitable for the synthesis of large-scale antenna arrays. However, the performance of the algorithm was not comprehensively analyzed. Noaman et al. [42] used a hybrid adaptive genetic algorithm (HAGA) to achieve the minimum SLL and control the nulls to obtain the desired beam patterns. Jayaprakasam et al. [43] proposed a hybrid swarm intelligence optimization algorithm called the particle swarm optimization and gravitational search algorithm-explore (PSOGSA-E) to achieve SLL suppression in collaborative beamforming. Roy et al. [44] developed a modified IWO algorithm to design the non-uniform circular antenna arrays. However, the number of the antenna elements is too small to give convincing results. Zhang et al. [45] used an improved IWO method to achieve better beam patterns of the time-modulated antenna arrays. However, the robustness of the proposed method is not evaluated. Liu et al. [46] developed a modified IWO algorithm to synthesize the beam patterns of phase-only reconfigurable LAAs, and they achieve superior results compared to some other approaches. However, the stability of this algorithm is not reported. Moreover, Majumdar et al. [47] proposed a quantized IWO algorithm to achieve desired beam patterns by digital phase shifters, but the efficiency of this algorithm is not verified.

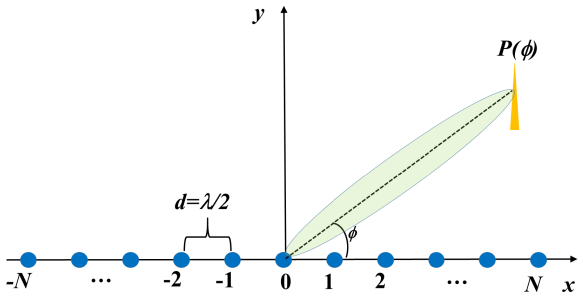

FIGURE 1. Geometry of $2N + 1$ isotropic antenna elements in an LAA.

III. GEOMETRIC STRUCTURES AND ARRAY FACTORS

The geometry structures of LAA and CAA and their array factors (AFs) are presented in this section.

A. LAA

The LAA is a kind of antenna array with the simplest fabrication and implementation [6]. Fig. 1 shows $2N + 1$ elements of an LAA; they are symmetrically placed on the x-axis. Moreover, the elements of the LAA are regarded as isotropic radiators. Thus, according to the principle of electromagnetic wave superposition, the AF of an LAA is given as follows [22]:

$$AF_{LAA}(\phi) = \sum_{n=-N}^{N} I_n^{LAA} \cos\left[kx_n \cos(\phi) + \varphi_n\right] \qquad (1)$$

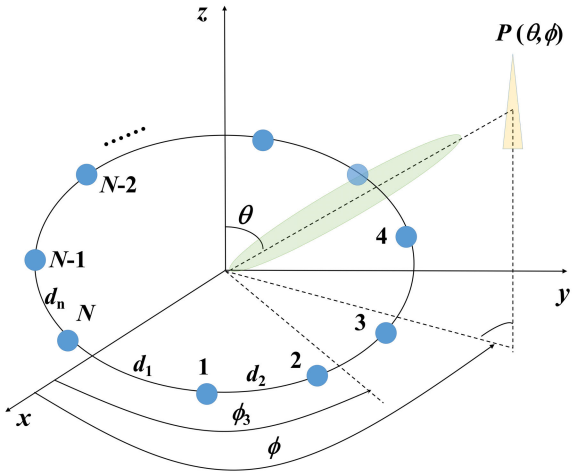

FIGURE 2. Geometry of *N* isotropic antenna elements in a uniform CAA.

where I_n^{LAA} is the excitation current of the nth element in LAA, k is the number of waves, φ_n is the phase of the nth element, ϕ is the azimuth angle measured from the positive x axis, and x_n is the location of the nth element.

B. CAA

As shown in Fig. 2, the number of isotropic antenna elements is N, and they are placed in the x-y plane ($\theta = 90°$), which make up the geometry of a CAA. These elements are uniformly distributed in a ring with a radius of a. Moreover, θ and ϕ represent the elevation angle measured from the z-axis and the azimuth angle measured from the positive x-axis, respectively. Similar to the LAA, we also assume the elements of the CAA to be isotropic radiators. Eq. (2) expresses the AF of a CAA [48]:

$$AF_{CAA}(\theta,\phi) = \sum_{n=1}^{N} I_n^{CAA}(jka[\sin(\theta)\cos(\phi-\phi_n) - \sin(\theta_0)\cos(\phi_0-\phi_n)]) \quad (2)$$

$$ka = \frac{2\pi}{\lambda}a = \sum_{i=1}^{N} d_i \quad (3)$$

$$\phi_n = \frac{2\pi\sum_{i=1}^{n} d_i}{ka} \quad (4)$$

where I_n^{CAA} is the excitation current of the nth element in CAA, and ϕ_n is the angular position of the nth element. λ is the wavelength, and d_i is the arc distance between the ith and $(i-1)$th elements. Moreover, ϕ_0 and θ_0 are set to be 0° and 90°, respectively.

IV. PROBLEM FORMULATION

In this work, we have two beam pattern optimization cases. The first one is to reduce the maximum SLLs of beam patterns, and the second one is to jointly optimize the maximum SLL and mainlobe beamwidth.

A. CASE ONE: MAXIMUM SLL REDUCTION

The first goal of this research is to reduce the maximum SLLs of LAAs and CAAs, respectively, and this can be achieved by predefining an optimal set of excitation currents. Thus, we propose the objective function and formulate the optimization problem as follows:

$$\begin{aligned} \min \quad & f = 10\log_{10}\frac{|AF(\phi_{MSL})|}{|AF(\phi_{ML})|} \\ \text{s.t.} \quad & \phi_{ML} = \arg\max|AF(\phi)|, \quad \phi \in [-\pi,\pi] \\ & \phi_{MSL} \in \max([-\pi,\phi_{FN1}]\cup[\phi_{FN2},\pi]) \\ & 0 \leqslant I_n \leqslant 1 \end{aligned} \quad (5)$$

where ϕ_{ML} and ϕ_{MSL} represent the angles of the mainlobe and maximum sidelobe, respectively. ϕ_{FN1} and ϕ_{FN2} represent the first nulls in $(-\pi,\phi_{FN1})$ and $(-\pi,\phi_{FN2})$, respectively; furthermore, they determine the first null beamwidth (FNBW) of the beam pattern. For the restrictive conditions, the location of mainlobe is defined by the first constraint, the range of sidelobe is shown in the second constraint, and the scope of normalized excitation current of each element is determined by the last constraint. In the fitness function shown in Eq. (5), the denominator can be regarded as a positive fix value since it represents the power of mainlobe. Thus, if the numerator of Eq. (5) which is the maximum SLL can be reduced, the minimized value of the fitness function can be achieved. Then, the lower maximum SLL can be obtained by searching for a better solution (excitation current) of the fitness function f. Moreover, during the optimization process, AF will be instantiated to AF_{LAA} and AF_{CAA}, respectively, for the SLL suppression optimizations of LAA and CAA.

B. CASE TWO: JOINT OPTIMIZATION OF MAXIMUM SLL AND MAINLOBE BEAMWIDTH

The second goal is to jointly achieve the maximum SLL and mainlobe beamwidth reductions of LAAs and CAAs, which is essentially a multi-objective optimization problem. Similar to case one, the excitation current value of each element can be predefined to achieve these two objectives. We use the linear weighting method to design the objective function and the joint optimization problem can be formulated as follows:

$$\begin{aligned} \min \quad & f = \underbrace{10\log_{10}\frac{|AF(\phi_{MSL})|}{|AF(\phi_{ML})|}}_{\text{Maximum SLL reduction}} + \underbrace{|\phi_{FN2}-\phi_{FN1}|}_{\text{Mainlobe beamwidth reduction}} \\ \text{s.t.} \quad & \phi_{ML} = \arg\max|AF(\phi)|, \quad \phi \in [-\pi,\pi] \\ & \phi_{MSL} \in \max([-\pi,\phi_{FN1}]\cup[\phi_{FN2},\pi]) \\ & 0 \leqslant I_n \leqslant 1 \end{aligned} \quad (6)$$

where the first item on the right is to reduce the maximum SLL, which is similar to case one, and the second item is used to simultaneously reduce the mainlobe beamwidth.

V. IWORMLF

A. CONVENTIONAL INVASIVE WEED OPTIMIZATION

Invasive weed optimization (IWO), which is a numerical stochastic optimization algorithm inspired by weed colonization, was first introduced by Mehrabian and Lucas in 2006 [49]. It is shown that this optimizer can not only be used to solve new electromagnetic optimization problems, but it also outperforms some other optimizers such as the PSO algorithm in certain instances. In IWO, a certain number of weeds make up the whole population, and each weed comprises a set of decision variables. Weeds are a serious threat to desirable plants because they are plants that are invasive and hardy.

Inspired from the colonizing behavior of weed plants, the process of the IWO algorithm includes three stages: reproduction, spatial dispersal, and competitive exclusion. All of the weeds (a solution of the problem is called a weed) in IWO participate in the process of reproduction. However, the fertilities of different weeds are not equivalent. The number of seeds produced by a weed is based on its fitness value. In a minimization problem, the weed that has the largest fitness function value generates fewer seeds. On the contrary, the weed with the smallest fitness function value generates more seeds. Therefore, the number of generated seeds varies as the fitness value changes in the colony. Moreover, the seeds of a weed are randomly dispersed in the search area in the same way as a normal distribution with mean zero and varying standard deviations [31]. After reproduction and spatial dispersal, the seeds and weeds enter a competition, and the winners are considered as weeds for the next generation.

The main steps of IWO are as follows:

Step 1: Initialization. The algorithm initializes a set of weeds that can be regarded as candidate solutions. These weeds are being randomly dispersed over the defined solution space.

Step 2: Reproduction. In this procedure, each solution in the population generates seeds based on the lowest and highest values of the fitness function in the search area. Eq. (7) gives the number of seeds generated by a weed:

$$S_{num} = floor\left[S_{\min} + (S_{\max} - S_{\min}) \times \frac{f - f_{worst}}{f_{best} - f_{worst}}\right] \quad (7)$$

where floor is the round down operation. $S_{\max}$ and $S_{\min}$ represent the maximum and minimum number of seeds, respectively, f represents the value of the fitness function of a weed. Moreover, f_{best} and f_{worst} are the best and worst values of the fitness function in a certain iteration, respectively.

Step 3: Spatial dispersal. In the d-dimensional defined solution space, there are new seeds that are randomly distributed in the surrounding of their parent weeds in the normal distribution with mean zero and varying standard deviations. Moreover, the new seeds grow to become new weeds. The standard deviation at this step is shown in Eq. (8), and Eq. (9) expresses the generation of new weeds as follows:

$$\sigma_{iter} = \frac{(iter_{\max} - iter)^m}{(iter_{\max} - 1)^m} \times (\sigma_{initial} - \sigma_{final}) + \sigma_{final} \quad (8)$$

Algorithm 1 IWORMLF

(1) Initialize a population of N weeds and define the related parameters;
(2) Calculate the fitness of each weed;
(3) Initialize X^*; // The best individual with the lowest fitness value;
for $t = 1$ *to* $iter_{max}$ **do**
  for $i = 1$ *to* N **do**
    Apply a random operator in the individual using Algorithm 2;
    if *new individual is better than previous* **then**
      update it;
      else
        keep the individual the same;
      end
    end
  end
  Select the f_{worst} and f_{best} in the mutant population by sorting;
  Generate new seeds: calculate S_{num} in the reproduction using Eq. (7);
  Distribute the seeds in the spatial distribution with the Lévy flight mechanism using Algorithm 3;
  Calculate the fitness of the new population;
  Eliminate individuals with higher fitness value in the colony to reach N;
  Update X^* if there is a better solution;
end
Return X^*.

$$W_{new}^{iter+1} = P^{iter} + N(0, \sigma_{iter}^2) \quad (9)$$

where σ_{final} and $\sigma_{initial}$ represent the predefined final and initial standard deviations, respectively. $iter$ represents the current iteration, $iter_{max}$ represents the maximum iteration, m represents the nonlinear modulation index, and P^{iter} defines the individual representing the parent weeds at the $iter$th iteration. W_{new}^{iter+1} is a weed generated from the individual at the $(iter + 1)$ iteration. $N(0, \sigma_{iter}^2)$ is a random number generated from the normal distribution with mean zero and standard deviation (SD).

Step 4: Competitive exclusion. After growth and reproduction, the number of weeds in the solution space will go beyond the upper limit of the number of individuals. Thus, weeds with lower ranking are eliminated to reach the limited number of individuals in the solution space. Then, the surviving ones will produce new seeds based on their ranking in the next iteration.

B. IMPROVED IWO

An IWORMLF approach with two improved factors is proposed to enhance the performance of the conventional IWO algorithm further. The pseudo code of the proposed algorithm is shown in Algorithm 1, and the details of the introduced improved factors are as follows:

1) RANDOM MUTATION OPERATOR

The standard deviation values of the seed dispersion in the conventional IWO are the same at a certain iteration, and decrease as a function of the number of iterations. Therefore, the convergence rate is largely limited. In IWO, the variance affects the exploration ability of the seeds directly. When the variance tends to be lower as the iteration increases, the global search ability of the algorithm will be decreased. Therefore, we propose a random mutation operator to mutate some individuals before the reproduction, thus enhancing the diversity of the population. The pseudo code of the process of the mutation operation is shown in Algorithm 2, and the random mutation operator is defined as follows:

$$P^{iter} = P^{iter} + R \times K \tag{10}$$

$$R = rand \times (P_m^{iter} - P_n^{iter}) \tag{11}$$

$$\begin{cases} K = 1, & rand(size(pop)) > pa \\ K = 0, & rand(size(pop)) \leq pa \end{cases} \tag{12}$$

where P_m^{iter} and P_n^{iter} are the two different individuals selected randomly in the population, R is the mutation factor, and *rand* is a random number generated from 0 to 1. Moreover, *pa* is the threshold parameter initialized as 0.25, *pop* is the population matrix, and K is a logical judgment factor whose value depends on *pa*. After the mutation process, a new population of the algorithm is obtained.

Algorithm 2 Random Mutation Operator

```
for i = 1 to N do
    Generate random number rand;
    if rand > pa then
        Select two different individuals: P_m^iter and P_n^iter;
        Calculate the difference ΔP between P_m^iter and P_n^iter;
        Mutate the individual P^iter according to ΔP using Eq. (10);
        else
            Keep the individual the same;
        end
    end
    Check if individual goes beyond value range and modify it;
    Calculate the fitness of individual;
end
Return mutant population.
```

2) LÉVY FLIGHT MECHANISM

The Lévy flight mechanism is utilized as the globe search operator in the spatial dispersal process, to improve the search efficiency of the algorithm. The pseudo code of the specific process of the introduced Lévy flight mechanism is shown in Algorithm 3, and the solution update method using this operator is as follows:

$$W_{new}^{iter+1} = P^{iter} + N(0, \sigma_{iter}^2) + Lévy(\beta) \tag{13}$$

$$Lévy(\beta) = L_{stepsize} \times N_{randn} \tag{14}$$

$$L_{stepsize} = \alpha \times \left\{ \frac{N_{randn}}{[abs(N_{randn})]^{\frac{1}{\beta}}} \times \frac{\Gamma(1+\beta) \times \sin(\frac{\pi}{2} \times \beta)}{[\Gamma(\frac{1+\beta}{2}) \times \beta \times 2^{(\frac{\beta-1}{2})}]^{\frac{1}{\beta}}} \right\} \times (P^{iter} - 0.5) \tag{15}$$

where $L_{stepsize}$ is the step length of the Lévy flight mechanism, α is the weight factor, N_{randn} is the random number. Compared with Eq. (9), we can see that the value of the weed generated in the next generation depends on their parent weeds and the $L_{stepsize}$. In this way, the global search performance of the algorithm can be enhanced.

Algorithm 3 Lévy Flight Mechanism

```
for i = 1 to N do
    for S = 1 to S_num do
        Calculate L_stepsize according to P^iter using Eq. (15);
        Distribute seeds according to the L_stepsize using Eq. (13);
        Check if any individual goes beyond the value range and modify it;
    end
end
Return the new weed population.
```

C. SIDELOBE SUPPRESSION USING IWORMLF

We used the proposed IWORMLF algorithm to optimize the beam pattern of the antenna arrays, and consider the candidate solutions (weeds) of the algorithm as the excitation currents of the elements. The solutions to the proposed optimization problem can be expressed as follows:

$$x = (I_1, I_2, I_3, \cdots, I_n) \tag{16}$$

where n represents the number of antenna elements. In addition, the population of IWORMLF is as follows:

$$pop = \begin{bmatrix} x_1 \\ x_2 \\ \cdots \\ x_N \end{bmatrix} = \begin{bmatrix} I_1^1 & I_2^1 & I_3^1 & \cdots & I_n^1 \\ I_1^2 & I_2^2 & I_3^2 & \cdots & I_n^2 \\ & & \cdots & & \\ I_1^N & I_2^N & I_3^N & \cdots & I_n^N \end{bmatrix} \tag{17}$$

where N is the population size.

VI. SIMULATIONS AND ANALYSIS

Matlab was used to simulate the process of synthesizing the beam pattern in order to suppress the maximum SLLs of the LAA and CAA. The computer used for the simulations had a Windows 10 operating system, 8 GB of RAM, and an Intel (R) Core (TM) i3-8100 CPU. Firstly, the performance of the proposed IWORMLF algorithm was tested in the standard benchmark functions, and the results were compared with

TABLE 1. Comparison of results of F_1, F_3, and F_4 for 30 independent runs.

ID	Algorithm	Best	Worst	Standard Deviation	Mean	Time
F_1	PSO	6.7707E+02	1.3242E+05	0.0000E+00	3.2109E+04	1.9997E+00
	BBO	2.2470E+06	6.7031E+07	0.0000E+00	2.6875E+07	7.4712E+01
	FA	4.5058E+09	4.5062E+09	0.0000E+00	4.5059E+09	4.2170E+00
	CS	1.1516E+08	1.9917E+09	0.0000E+00	9.0359E+08	2.0265E+00
	IWO	1.2652E+07	1.1366E+09	0.0000E+00	1.7474E+08	1.8466E+00
	CDA	4.5058E+09	4.5246E+09	3.4381E+06	4.5071E+09	9.0704E+00
	IWOA	4.5058E+09	4.5371E+09	5.7067E+06	4.5076E+09	7.2326E-01
	IDHS	4.5058E+09	4.5058E+09	0.0000E+00	4.5058E+09	2.1432E+00
	IWORMLF	1.0714E+06	1.2441E+07	0.0000E+00	4.2554E+06	9.6445E+00
F_3	PSO	3.0294E+02	1.8545E+04	0.0000E+00	3.1947E+03	1.9223E+00
	BBO	1.1125E+03	2.6326E+04	0.0000E+00	9.4452E+03	7.5636E+01
	FA	2.3578E+06	2.3578E+06	0.0000E+00	2.3578E+06	4.2516E+00
	CS	9.6583E+04	2.3578E+06	0.0000E+00	1.7541E+06	2.0301E+00
	IWO	1.3268E+04	1.1408E+05	0.0000E+00	5.0833E+04	1.8956E+00
	CDA	2.3578E+06	2.3579E+06	3.1331E+01	2.3579E+06	8.6765E+00
	IWOA	2.3578E+06	2.3578E+06	3.8696E+00	2.3578E+06	6.8177E-01
	IDHS	2.3578E+06	2.3578E+06	4.7362E-10	2.3578E+06	2.1045E+00
	IWORMLF	1.3906E+03	9.6552E+03	0.0000E+00	**2.5151E+03**	1.0249E+01
F_4	PSO	4.0001E+02	4.3478E+02	0.0000E+00	4.2587E+02	1.9249E+00
	BBO	4.0105E+02	5.2564E+02	0.0000E+00	4.4179E+02	7.5063E+01
	FA	1.1775E+04	1.1777E+04	0.0000E+00	1.1775E+04	4.0495E+00
	CS	1.8543E+03	1.1775E+04	0.0000E+00	6.3787E+03	2.0293E+00
	IWO	7.1125E+02	5.7884E+03	0.0000E+00	2.7893E+03	1.8294E+00
	CDA	1.1775E+04	1.1825E+04	1.4660E+01	1.1794E+04	9.1373E+00
	IWOA	1.1775E+04	1.1858E+04	2.4141E+01	1.1788E+04	6.8485E-01
	IDHS	1.1775E+04	1.1775E+04	5.5503E-12	1.1775E+04	2.1424E+00
	IWORMLF	4.0984E+02	4.7042E+02	0.0000E+00	4.3036E+02	9.2743E+00

PSO, BBO, FA, CS, and IWO, which are classical evolutionary algorithms. Moreover, three recently proposed algorithms that are CDA, IWOA and IDHS were also introduced for comparison. Secondly, we tune the important parameters that control the performance of the proposed IWORMLF algorithm. The appropriate value of parameters can make the IWORMLF algorithm achieve the best performance for SLL reduction optimization. Thirdly, we used IWORMLF as well as the above-mentioned algorithms to solve the formulated optimization problem in order to synthesize the beam pattern. Fourthly, the stability of the proposed IWORMLF was evaluated. Then, the effectiveness of the two introduced improved factors was verified by performing simulations. Finally, we conduct EM simulations to evaluate the effectiveness of the proposed IWORMLF for the beam pattern synthesis when considering the mutual coupling between the elements.

A. PERFORMANCE ANALYSIS OF IWORMLF

Before solving the formulated SLL reduction optimization problem, we performed a comparative experiment to test the overall performance of the proposed IWORMLF algorithm. We adopted the IWORMLF and other algorithms to obtain the minimum values of nine selected functions (i.e., F_1, F_3, F_4, F_6, F_{20}, F_{22}, F_{24}, F_{25}, and F_{26}) of the standard CEC 2014 function set [50]. This is a common test function set for evaluating the performance of the swarm intelligence and evolutionary algorithms. Thus, the test results are convincing since it can be compared to other approaches and previous work. Moreover, the nine selected functions are with different characteristics. For example, F_1 and F_3 are unimodal functions, F_4 and F_6 are simple multimodal functions, F_{20} and F_{22} are hybrid functions, and F_{24}, F_{25} and F_{26} are composition functions. These selected test function cover all function types in the test set, so it can be regarded as a comprehensive performance test for the proposed algorithm.

The dimension of the solution, the population size, and the maximum number of iterations of each algorithm were set to 10, 20, and 1000, respectively. Moreover, the tests were independently run 30 times on each function, and the statistical results are shown in Tables 1, 2, and 3, respectively. As can be seen in the tables, the proposed IWORMLF algorithm achieves the best results for six of the nine functions. Thus, the comparison results indicate that the proposed IWORMLF algorithm is expected to be a reliable choice for optimization problems.

B. TUNING OF PARAMETER VALUES

The optimal values of parameters in an optimization algorithm are different when solving different problems. Thus, the key parameters of the proposed IWORMLF algorithm need to be tuned so that the algorithm is able to achieve a better result for both of the formulated optimization problems. In the proposed IWORMLF, α is the most sensitive parameter, and it controls the step length of the Lévy flight mechanism. Thus, in this tuning test, we used IWORMLF to find the solutions for both the two formulated optimization problems by changing the values of α from 0.1 to 1.0, and the step size is set as 0.1. Moreover, the test was repeated 50 times to prevent random bias, and average values are presented. For the maximum SLL reductions, Figs. 3(a) and 3(b) show the tuning results of the beam pattern optimizations

TABLE 2. Comparison of results of F_6, F_{20}, and F_{22} for 30 independent runs.

ID	Algorithm	Best	Worst	Standard Deviation	Mean	Time
F_6	PSO	6.0061E+02	6.0566E+02	0.0000E+00	6.0244E+02	2.3527E+00
	BBO	6.0172E+02	6.0556E+02	0.0000E+00	6.0364E+02	1.0303E+02
	FA	6.1388E+02	6.1423E+02	0.0000E+00	6.1402E+02	4.7566E+00
	CS	6.1253E+02	6.1389E+02	0.0000E+00	6.1372E+02	3.9395E+00
	IWO	6.0943E+02	6.1595E+02	0.0000E+00	6.1349E+02	3.1772E+00
	CDA	6.1393E+02	6.1432E+02	9.8238E-02	6.1417E+02	9.0555E+00
	IWOA	6.1395E+02	6.1426E+02	5.7084E-02	6.1409E+02	1.2137E+00
	IDHS	6.1385E+02	6.1396E+02	2.6452E-02	6.1391E+02	2.5426E+00
	IWORMLF	6.0302E+02	6.0674E+02	0.0000E+00	6.0479E+02	9.6665E+00
F_{20}	PSO	2.0364E+03	2.8405E+04	5.4457E+03	6.7751E+03	1.8975E+00
	BBO	2.4144E+03	2.5465E+05	8.2667E+04	9.6198E+04	7.5912E+01
	FA	7.6699E+08	7.6699E+08	1.8809E-01	7.6699E+08	4.2464E+00
	CS	2.1173E+05	6.4027E+08	1.5314E+08	8.9024E+07	2.0801E+00
	IWO	3.5261E+03	6.1920E+06	1.2004E+06	4.8090E+05	1.9255E+00
	CDA	7.6699E+08	7.6699E+08	7.8618E+01	7.6699E+08	8.7204E+00
	IWOA	7.6699E+08	7.6700E+08	3.1661E+02	7.6699E+08	7.8019E-01
	IDHS	7.6699E+08	7.6699E+08	3.6374E-07	7.6699E+08	2.1366E+00
	IWORMLF	2.5134E+03	1.1676E+04	2.7216E+03	**6.6165E+03**	1.1035E+01
F_{22}	PSO	2.2218E+03	2.5313E+03	6.0636E+01	2.3392E+03	1.9343E+00
	BBO	2.2214E+03	2.5123E+03	9.2601E+01	2.3219E+03	7.7004E+01
	FA	1.0321E+04	1.0328E+04	3.0452E+00	1.0325E+04	4.2471E+00
	CS	2.6274E+03	5.3810E+03	4.9604E+02	3.1600E+03	2.1607E+00
	IWO	2.3955E+03	3.3709E+03	2.3264E+02	2.7523E+03	2.0272E+00
	CDA	1.0321E+04	1.0365E+04	7.4823E+00	1.0328E+04	8.6525E+00
	IWOA	1.0322E+04	1.0395E+04	1.7815E+01	1.0330E+04	7.3306E-01
	IDHS	1.0321E+04	1.0327E+04	2.9300E+00	1.0324E+04	2.1629E+00
	IWORMLF	2.2315E+03	2.3694E+03	5.3356E+01	**2.2724E+03**	9.1370E+00

TABLE 3. Comparison of results of F_{24}, F_{25} and F_{26} for 30 independent runs.

ID	Algorithm	Best	Worst	Standard Deviation	Mean	Time
F_{24}	PSO	2.5136E+03	2.6093E+03	3.3589E+01	2.5552E+03	1.9638E+00
	BBO	2.6000E+03	2.6000E+03	0.0000E+00	2.6000E+03	7.9806E+01
	FA	2.6000E+03	2.6004E+03	8.1980E-02	2.6000E+03	4.1977E+00
	CS	2.6000E+03	2.6000E+03	0.0000E+00	2.6000E+03	2.3292E+00
	IWO	2.5474E+03	2.6577E+03	2.7999E+01	2.6258E+03	2.1929E+00
	CDA	2.6000E+03	2.6010E+03	3.3007E-01	2.6004E+03	8.1991E+00
	IWOA	2.6000E+03	2.6000E+03	0.0000E+00	2.6000E+03	8.9850E-01
	IDHS	2.6001E+03	2.6005E+03	9.8967E-02	2.6003E+03	2.2014E+00
	IWORMLF	2.5229E+03	2.6003E+03	2.4071E+01	**2.5467E+03**	9.0220E+00
F_{25}	PSO	2.6323E+03	2.7035E+03	1.4671E+01	2.6941E+03	1.9848E+00
	BBO	2.7000E+03	2.7000E+03	0.0000E+00	2.7000E+03	8.0451E+01
	FA	2.7000E+03	2.7000E+03	0.0000E+00	2.7000E+03	3.9795E+00
	CS	2.7000E+03	2.7000E+03	0.0000E+00	2.7000E+03	2.3755E+00
	IWO	2.6972E+03	2.7282E+03	6.4659E+00	2.7100E+03	2.2191E+00
	CDA	2.7000E+03	2.7000E+03	0.0000E+00	2.7000E+03	8.4466E+00
	IWOA	2.7000E+03	2.7000E+03	0.0000E+00	2.7000E+03	8.3935E-01
	IDHS	2.7000E+03	2.7000E+03	0.0000E+00	2.7000E+03	2.1496E+00
	IWORMLF	2.6511E+03	2.7027E+03	1.5243E+01	**2.6930E+03**	8.9185E+00
F_{26}	PSO	2.7001E+03	2.8000E+03	2.5318E+01	2.7069E+03	2.5339E+00
	BBO	2.7002E+03	2.7012E+03	2.0903E-01	2.7005E+03	1.1258E+02
	FA	2.8000E+03	2.8000E+03	0.0000E+00	2.8000E+03	4.6012E+00
	CS	2.7028E+03	2.8000E+03	3.7847E+01	2.7303E+03	4.3817E+00
	IWO	2.7018E+03	2.8034E+03	2.4995E+01	2.7110E+03	4.2081E+00
	CDA	2.8000E+03	2.8000E+03	2.2125E-04	2.8000E+03	8.7952E+00
	IWOA	2.8000E+03	2.8000E+03	0.0000E+00	2.8000E+03	1.3924E+00
	IDHS	2.8000E+03	2.8000E+03	0.0000E+00	2.8000E+03	2.6511E+00
	IWORMLF	2.7002E+03	2.7006E+03	8.8337E-02	**2.7004E+03**	9.8192E+00

of 64-element LAA and CAA, respectively. As shown in the figures, the optimal values of α are 0.6 and 0.1, respectively. For joint sidelobe and mainlobe beamwidth reductions, the parameter tuning results of LAA and CAA beam pattern optimizations are shown in Figs. 4(a) and 4(b). It can be seen from the figures that the optimal values of α for these cases are 0.6 and 0.4, respectively.

In addition, the previous study provides parametric values for other algorithms. For PSO [51], we used the following parameters: first learning factor $C1 = 1.5$, and second learning factor $C2 = 2.0$. For BBO [52], the immigration rate $I = 1$, emigration rate $E = 1$, and mutation rate $r = 0.005$. For FA [53], the randomization parameter $\alpha = 0.25$, attractiveness $\beta_0 = 0.2$, and absorption coefficient $\gamma = 0.25$. For

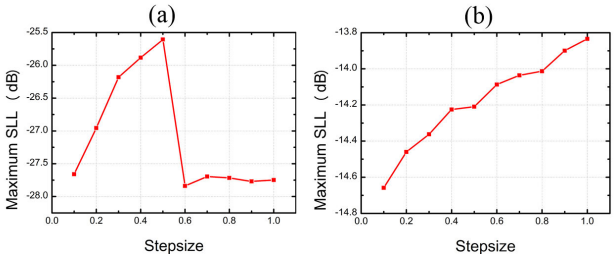

FIGURE 3. Parameter tuning for α in IWORMLF for maximum SLL reduction. (a) 64-element LAA. (b) 64-element CAA.

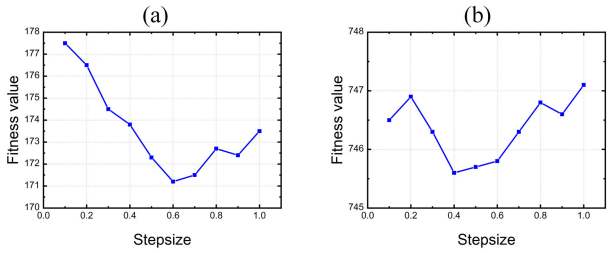

FIGURE 4. Parameter tuning for α in IWORMLF for joint sidelobe and mainlobe beamwidth reduction. (a) 64-element LAA. (b) 64-element CAA.

TABLE 4. Parameter setups of different algorithms.

Algorithm	Values of parameters
PSO [52]	$C1 = 1.5, C2 = 2.0$
BBO [53]	$I = 1, E = 1, r = 0.005$
FA [54]	$\alpha = 0.25, \beta_0 = 0.2, \gamma = 0.25$
CS [55]	$p_a = 0.25, \alpha = 1$
IWO [31]	$S_{max} = 5, S_{min} = 0, m = 3,$ $\sigma_{initial} = 0.05, \sigma_{final} = 0.01$
CDA [40]	$\beta = 1.5$
IWOA [36]	$a = [2, 0], b = 1,$ $Crossover\_ratio = 0.1,$ $beta\_min = 0.3, beta\_max = 0.7$
IDHS [38]	$PAR_{min} = 0.1, PAR_{max} = 0.9,$ $HMACR_{min} = 0.8, HMCR_{max} = 0.9$ $\sigma_{initial} = 0.05, \sigma_{final} = 0.01,$
IWORMLF	$S_{max} = 5, S_{min} = 0, m = 3, pa = 0.25$

CS [54], the probability that an egg is discovered $p_a = 0.25$, and the step size of Lévy flight $\alpha = 1$. For IWO [31], the minimum number of seeds $S_{min} = 0$, the maximum number of seeds $S_{max} = 5$, the initial standard deviation $\sigma_{initial} = 0.01$, the final standard deviation $\sigma_{final} = 0.05$, and the nonlinear modulation index $m = 3$. For CDA [39], a constant β in Lévy flight is 1.5. For IWOA [35], we used the crossover ratio $Crossover\_ratio = 0.1$, a decreased range $a = [2,0]$, and a constant to define the shape of the logarithmic spiral $b = 1$. For IDHS [37], the pitch adjusting rates PAR_{min} and PAR_{max} are set to 0.1 and 0.9, respectively, and the harmony memory considering rates $HMCR_{min}$ and $HMCR_{max}$ are 0.8 and 0.9, respectively.

The parameter setups of the proposed IWORMLF and the values of all parameters used in other algorithms are shown in Table 4.

C. BEAM PATTERN SYNTHESIS OF LAA

In this part, the proposed IWORMLF algorithm is adopted to solve the two formulated optimization problems in several samples with different numbers of elements, and the above-mentioned approaches are also adopted as the comparison algorithms.

Moreover, the tests are repeated independently for 50 times to avoid random bias. Note that the beam patterns and convergence rates shown in this section are the median and average results of the 50 tests.

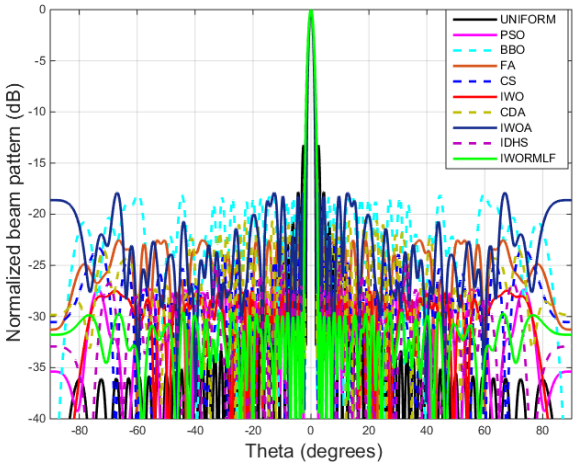

FIGURE 5. 2D beam patterns of 64-element LAA obtained by different algorithms for reducing the maximum SLL.

TABLE 5. Maximum SLLs and mainlobe beamwidth obtained by different algorithms for example 1.

	Maximum SLL (dB)	Mainlobe beamwidth (degree)
Uniform	-13.2447	3.5019
PSO	-27.3533	5.1028
BBO	-18.0544	4.1023
FA	-22.5400	4.9027
CS	-22.9651	4.5025
IWO	-27.4473	5.3029
CDA	-20.5844	4.1023
IWOA	-17.8971	4.1023
IDHS	-24.8950	5.5031
IWORMLF	-29.5521	5.3029

1) EXAMPLE 1: BEAM PATTERN SYNTHESIS OF 64-ELEMENT LAA FOR MAXIMUM SLL REDUCTION

Fig. 5 shows the two-dimension (2D) beam patterns that belong to the 64-element LAA synthesized by PSO, BBO, FA, CS, IWO, CDA, IWOA, IDHS and the proposed IWORMLF for reducing the maximum SLL. Moreover, the result of the uniform array is also shown in the figure. Note that for each antenna element in the uniform array, the excitation current is set to 1. Correspondingly, the numerical statistical results of the maximum SLLs and mainlobe beamwidth obtained by abovementioned algorithms are listed in Table 5. It can be seen from the figure and table that the proposed IWORMLF algorithm achieves the lowest maximum SLL of -29.5521 dB among all the algorithms. Moreover, the convergence rates of different approaches in the optimization process are shown in Fig. 6. As can be seen, IWORMLF has the best performance from the perspectives of accuracy

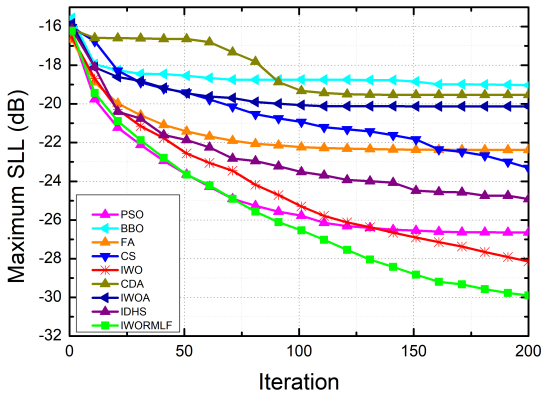

FIGURE 6. Convergence rates of different algorithms for reducing the maximum SLL of 64-element LAA.

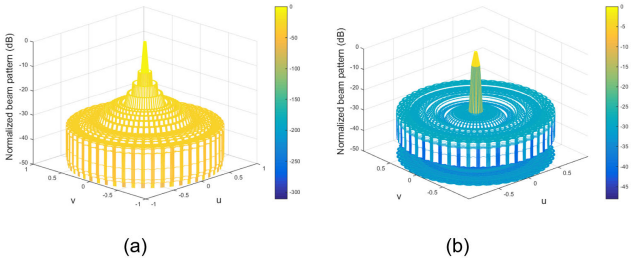

FIGURE 7. 3D beam patterns of 64-element LAA obtained by different approaches for reducing the maximum SLL. (a) Uniform LAA. (b) IWORMLF.

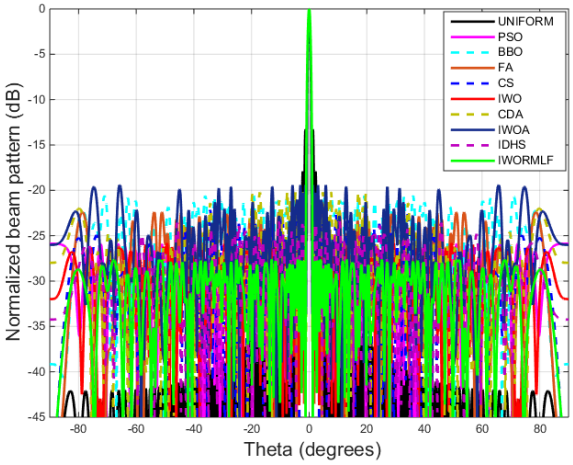

FIGURE 8. 2D beam patterns of 128-element LAA obtained by different algorithms for reducing the maximum SLL.

and convergence rate. In addition, the three-dimension (3D) beam patterns obtained by the uniform LAA and IWORMLF are shown in Figs. 7(a) and 7(b), respectively, for a intuitive comparison. As can be seen, the maximum SLL is evidently suppressed after the optimization by the proposed approach.

2) EXAMPLE 2: BEAM PATTERN SYNTHESIS OF 128-ELEMENT LAA FOR MAXIMUM SLL REDUCTION

Figs. 8 and 9 show the 2D beam patterns and convergence rates obtained by different algorithms for the 128-element LAA, respectively. Moreover, the numerical statistical results

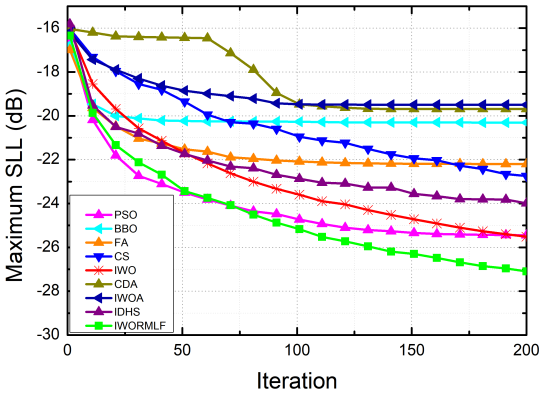

FIGURE 9. Convergence rates of different algorithms for reducing the maximum SLL of 128-element LAA.

TABLE 6. Maximum SLLs and mainlobe beamwidth obtained by different algorithms for example 2.

	Maximum SLL (dB)	Mainlobe beamwidth (degree)
Uniform	-13.2637	1.7009
PSO	-25.8730	2.5014
BBO	-20.5924	2.3013
FA	-22.3947	2.1012
CS	-22.0974	2.1012
IWO	-25.7756	2.5014
CDA	-20.2001	2.1012
IWOA	-19.4042	2.1012
IDHS	-23.4136	2.5014
IWORMLF	-27.5992	2.5014

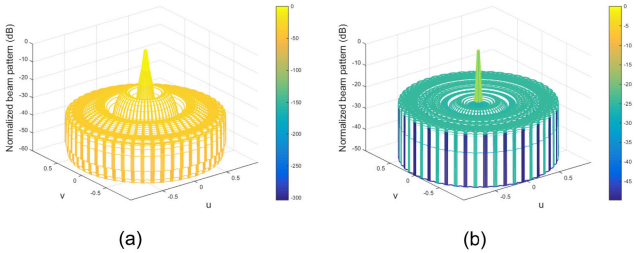

FIGURE 10. 3D beam patterns of 128-element LAA obtained by different approaches for reducing the maximum SLL. (a) Uniform LAA. (b) IWORMLF.

in terms of the maximum SLLs and mainlobe beamwidth are listed in Table 6. As can be seen, the proposed IWORMLF algorithm achieves the lowest maximum SLL of −27.5992 dB and faster convergence rate compared to other algorithms. Moreover, Figs. 10(a) and 10(b) show the 3D beam patterns synthesized by the uniform array and IWORMLF algorithm, respectively.

3) EXAMPLE 3: BEAM PATTERN SYNTHESIS OF 64-ELEMENT LAA FOR JOINTLY REDUCING THE MAXIMUM SLL AND MAINLOBE BEAMWIDTH

Fig. 11 shows the 2D beam patterns obtained by different algorithms for jointly reducing the maximum SLL and mainlobe beamwidth, and the convergence rates of different algorithms during the optimization process are shown

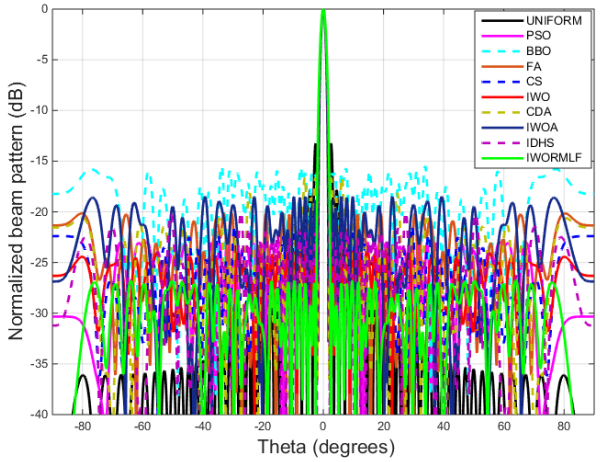

FIGURE 11. 2D beam patterns of 64-element LAA obtained by different algorithms for jointly reducing the maximum SLL and mainlobe beamwidth.

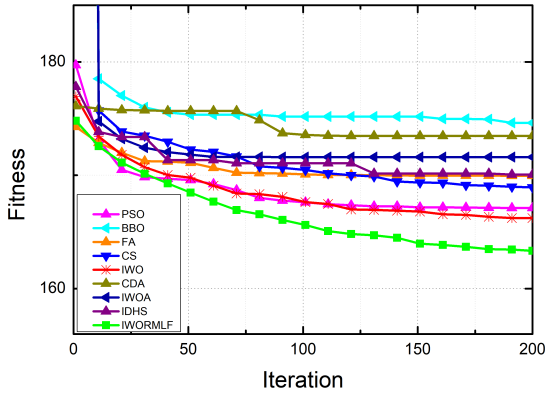

FIGURE 12. Convergence rates of different algorithms for jointly reducing the maximum SLL and mainlobe beamwidth of 64-element LAA.

TABLE 7. Maximum SLLs and mainlobe beamwidth obtained by different algorithms for example 3.

	Maximum SLL (dB)	Mainlobe beamwidth (degree)
Uniform	-13.2400	3.5019
PSO	-22.9795	4.9027
BBO	-15.4912	4.3024
FA	-20.1465	4.1023
CS	-21.1734	4.3024
IWO	-23.8728	4.7026
CDA	-16.6252	3.9022
IWOA	-18.4951	4.1023
IDHS	-20.0352	4.3024
IWORMLF	-26.7645	4.9027

in Fig. 12. Moreover, Table 7 shows the numerical statistical results of the maximum SLLs and mainlobe beamwidth obtained by different algorithms. It can be seen from these figures and tables that the proposed IWORMLF algorithm can achieve the lowest maximum SLL. However, the mainlobe beamwidth obtained by IWORMLF is not the lowest compared to some other algorithms. This is because that there are trade-offs between the sidelobe and mainlobe, which means that the reduced sidelobe will cause the increasing of

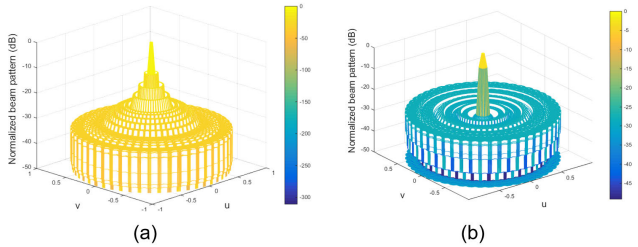

FIGURE 13. 3D beam patterns of 64-element LAA obtained by different approaches for jointly reducing the maximum SLL and mainlobe beamwidth. (a) Uniform LAA. (b) IWORMLF.

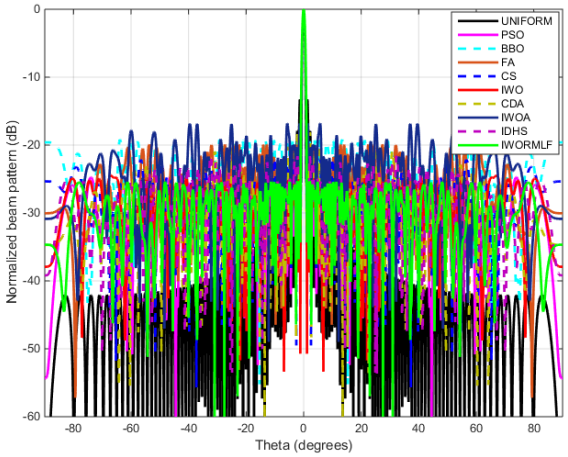

FIGURE 14. 2D beam patterns of 128-element LAA obtained by different algorithms for jointly reducing the maximum SLL and mainlobe beamwidth.

the mainlobe [55]. However, the mainlobe beamwidth gets narrow compare to the case that only reduces the maximum SLL shown in example 1, which indicate that the proposed IWORMLF algorithm is effective to achieve both maximum SLL and mainlobe beamwidth reductions. Moreover, the corresponding 3D beam patterns obtained by the uniform LAA and IWORMLF are shown in Figs. 13(a) and 13(b), respectively.

4) EXAMPLE 4: BEAM PATTERN SYNTHESIS OF 128-ELEMENT LAA FOR JOINTLY REDUCING THE MAXIMUM SLL AND MAINLOBE BEAMWIDTH

Figs. 14 and 15 show the beam patterns and convergence rates obtained by different algorithms for the joint reduction of maximum SLL and mainlobe beamwidth of the 128-element LAA, respectively. Similar to example 3, the numerical statistical results of the maximum SLLs and mainlobe beamwidth are presented in Table 8. As can be seen, the proposed IWORMLF achieves the best performance in terms of the maximum SLL reduction compared to other algorithms. Similar to the case of example 2, the proposed IWORMLF algorithm achieves the lowest maximum SLL of -25.2969 dB among all the algorithms, and the mainlobe beamwidth obtained by IWORMLF is not the best among all the algorithms due to the trade-offs

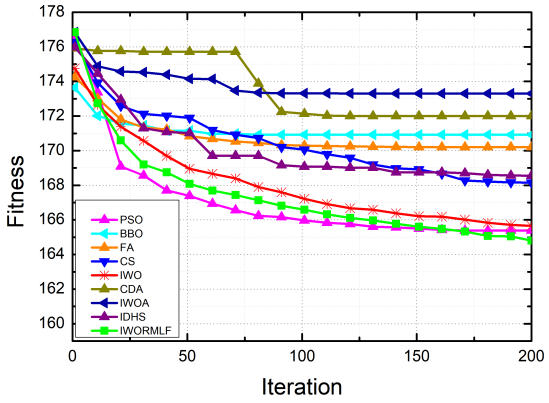

FIGURE 15. Convergence rates of different algorithms for jointly reducing the maximum SLL and mainlobe beamwidth of 128-element LAA.

TABLE 8. Maximum SLLs and mainlobe beamwidth obtained by different algorithms for example 4.

	Maximum SLL (dB)	Mainlobe beamwidth (degree)
Uniform	-13.2600	1.7009
PSO	-24.7227	2.3013
BBO	-19.1837	2.1012
FA	-19.9044	2.1012
CS	-21.9511	2.1012
IWO	-24.4494	2.3013
CDA	-18.1063	1.9011
IWOA	-16.7998	2.1012
IDHS	-21.5551	2.3013
IWORMLF	-25.2969	2.3013

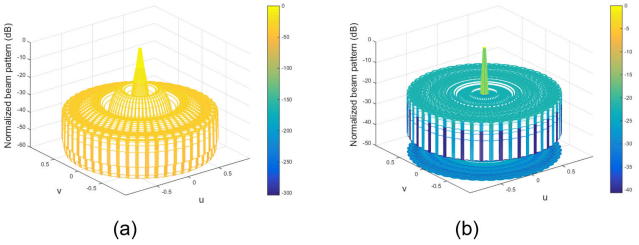

FIGURE 16. 3D beam patterns of 128-element LAA obtained by different approaches for jointly reducing the maximum SLL and mainlobe beamwidth. (a) Uniform LAA. (b) IWORMLF.

between the sidelobe and mainlobe. However, compared to the case that only considers to optimize the maximum SLL, the mainlobe beamwidth of each algorithm is significantly reduced. In addition, the 3D beam patterns obtained by uniform LAA and IWORMLF of 128-element case are shown in Figs. 16(a) and 16(b), respectively.

D. BEAM PATTERN SYNTHESIS OF CAA

In this section, the beam patterns of CAA with different numbers of antenna elements are optimized by IWORMLF and other comparison algorithms.

1) EXAMPLE 5: BEAM PATTERN SYNTHESIS OF 64-ELEMENT CAA FOR MAXIMUM SLL REDUCTION

Fig. 17 shows the 2D beam patterns of 64-element CAA obtained by the uniform array, PSO, BBO, FA, CS, IWO, CDA, IWOA, IDHS and the proposed IWORMLF, and the corresponding convergence rates of these approaches are shown in Fig. 18. Moreover, Table 9 shows the numerical statistical results of the maximum SLLs and mainlobe beamwidth achieved by different algorithms. It can be seen from the figures and tables that IWORMLF has the best performance for this optimization case. In addition, the 3D beam patterns of the uniform array and IWORMLF are shown

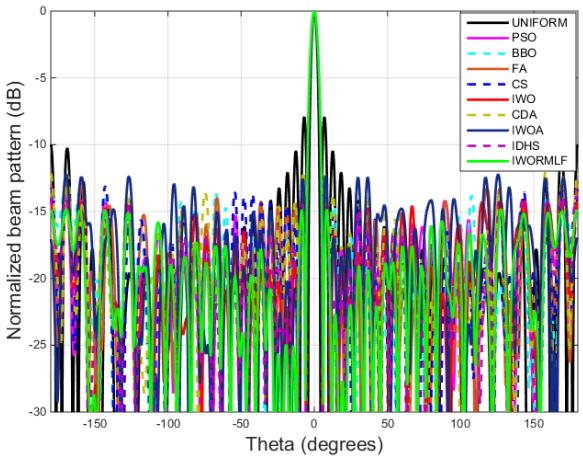

FIGURE 17. 2D beam patterns of 64-element CAA obtained by different algorithms for reducing the maximum SLL.

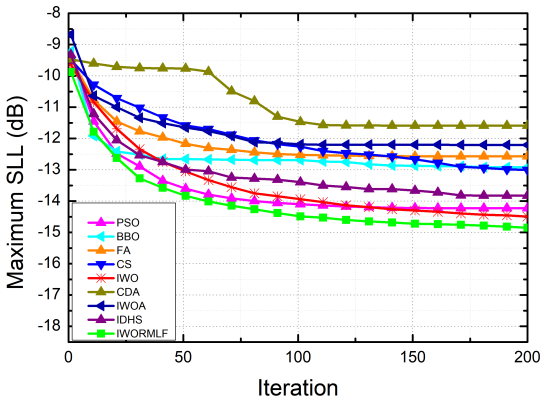

FIGURE 18. Convergence rates of different algorithms for reducing the maximum SLL of 64-element CAA.

TABLE 9. Maximum SLLs and mainlobe beamwidth obtained by different algorithms for example 5.

	Maximum SLL (dB)	Mainlobe beamwidth (degree)
Uniform	-7.9048	8.8000
PSO	-14.1282	11.2000
BBO	-13.5386	11.6000
FA	-12.9717	10.8000
CS	-13.0861	10.8000
IWO	-14.1828	11.6000
CDA	-11.9592	10.4000
IWOA	-12.1833	10.8000
IDHS	-13.8564	11.6000
IWORMLF	-14.8114	12.4000

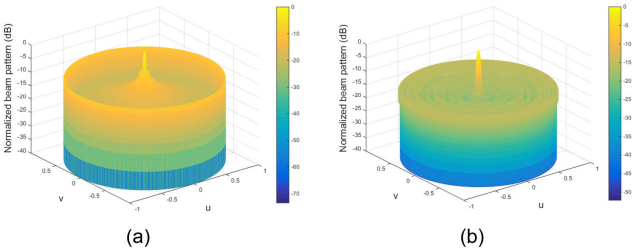

FIGURE 19. 3D beam patterns of 64-element CAA obtained by different approaches for reducing the maximum SLL. (a) Uniform LAA. (b) IWORMLF.

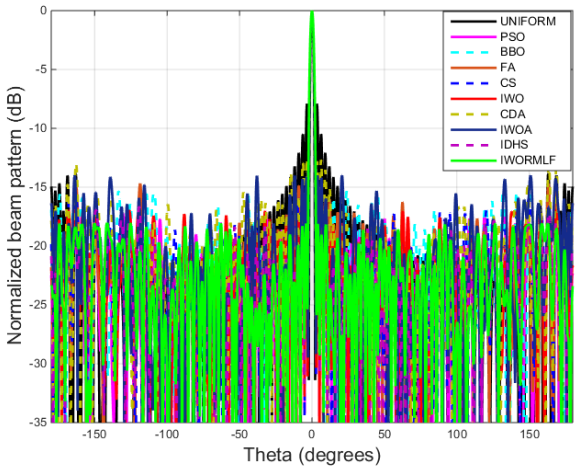

FIGURE 20. 2D beam patterns of 128-element CAA obtained by different algorithms for reducing the maximum SLL.

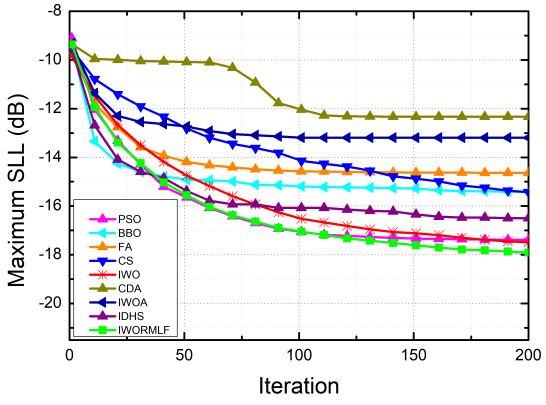

FIGURE 21. Convergence rates of different algorithms for reducing the maximum SLL of 128-element CAA.

in Figs. 19(a) and 19(b), respectively, for present the optimization results intuitively.

2) EXAMPLE 6: BEAM PATTERN SYNTHESIS OF 128-ELEMENT CAA FOR MAXIMUM SLL REDUCTION

Fig. 20 shows the 2D beam patterns of 128-element CAA obtained by different algorithms, and the convergence rates of these algorithms are shown in Fig. 21. Table 10 shows

TABLE 10. Maximum SLLs and mainlobe beamwidth obtained by different algorithms for example 6.

	Maximum SLL (dB)	Mainlobe beamwidth (degree)
Uniform	-7.9043	4.4000
PSO	-17.1654	6.0000
BBO	-15.2948	6.0000
FA	-14.6828	5.2000
CS	-15.8242	5.6000
IWO	-16.8898	6.0000
CDA	-12.5669	5.2000
IWOA	-13.9893	5.6000
IDHS	-16.6135	6.4000
IWORMLF	-18.0214	6.2000

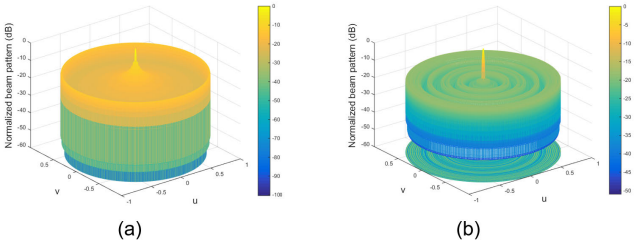

FIGURE 22. 3D beam patterns of 128-element CAA obtained by different approaches for reducing the maximum SLL. (a) Uniform CAA. (b) IWORMLF.

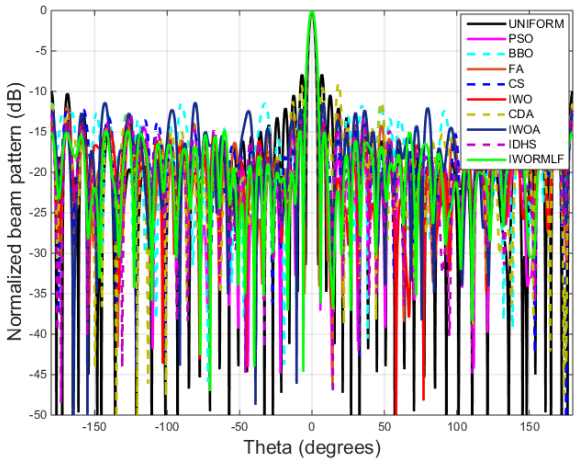

FIGURE 23. 2D beam patterns of 64-element CAA obtained by different algorithms for jointly reducing the maximum SLL and mainlobe beamwidth.

the numerical statistical results of the maximum SLLs and mainlobe beamwidth obtained by different methods. As can be seen, the proposed IWORMLF algorithm gets the average maximum SLL of -18.0214 dB, which is the lowest among all the introduced algorithms. Moreover, the 3D beam patterns of the uniform array and IWORMLF are shown in Figs. 22(a) and 22(b), respectively.

3) EXAMPLE 7: BEAM PATTERN SYNTHESIS OF 64-ELEMENT CAA FOR JOINTLY REDUCING THE MAXIMUM SLL AND MAINLOBE BEAMWIDTH

In this example, the 2D beam patterns of 64-element CAA obtained by different algorithms and the convergence rates of these algorithms are shown in Figs. 23 and 24, respectively,

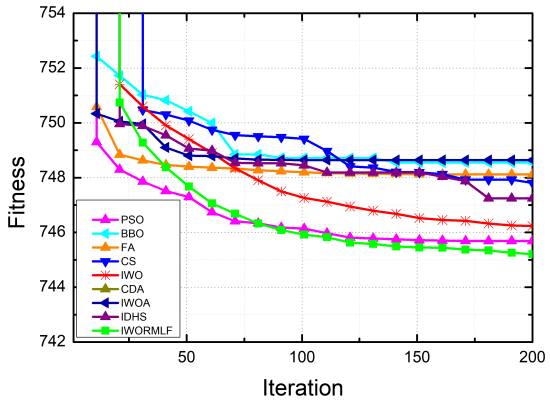

FIGURE 24. Convergence rates of different algorithms for jointly reducing the maximum SLL and mainlobe beamwidth of 64-element CAA.

TABLE 11. Maximum SLLs and mainlobe beamwidth obtained by different algorithms for example 7.

	Maximum SLL (dB)	Mainlobe beamwidth (degree)
Uniform	-7.9048	8.8000
PSO	-14.3141	11.6000
BBO	-11.4495	11.0000
FA	-11.8815	10.4000
CS	-12.1943	11.0000
IWO	-13.7691	11.6000
CDA	-9.0220	9.2000
IWOA	-11.3594	10.4000
IDHS	-12.7522	11.0000
IWORMLF	-14.7942	12.0000

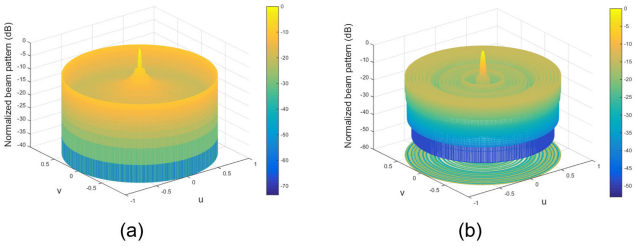

FIGURE 25. 3D beam patterns of 64-element CAA obtained by different approaches for jointly reducing the maximum SLL and mainlobe beamwidth. (a) Uniform CAA. (b) IWORMLF.

and the numerical statistical results of the maximum SLLs and mainlobe beamwidth are presented in Table 11. It can be seen from these results that proposed IWORMLF achieves the best performance in terms of the maximum SLL reduction, and the mainlobe beamwidth is the best compared to other approaches. Similar to the LAA cases, this is also because of the trade-offs between the mainlobe and sidelobe. However, it can be seen from Table 11 that the mainlobe beamwidth is reduced by using the joint optimization mechanism, which indicates the effectiveness of the proposed algorithm. Moreover, the 3D beam patterns obtained by the uniform array and the proposed IWORMLF are shown in Figs. 25(a) and 25(b), respectively.

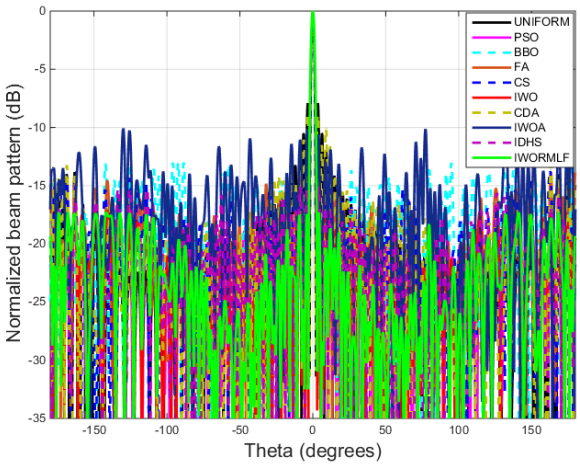

FIGURE 26. 2D beam patterns of 128-element CAA obtained by different algorithms for jointly reducing the maximum SLL and mainlobe beamwidth.

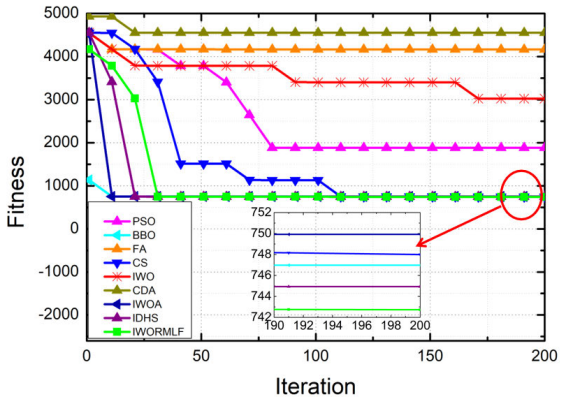

FIGURE 27. Convergence rates of different algorithms for jointly reducing the maximum SLL and mainlobe beamwidth of 128-element CAA.

4) EXAMPLE 8: BEAM PATTERN SYNTHESIS OF 128-ELEMENT CAA FOR JOINTLY REDUCING THE MAXIMUM SLL AND MAINLOBE BEAMWIDTH

Figs. 26 and 27 show the beam patterns and convergence rates obtained by different algorithms for the joint maximum SLL and mainlobe beamwidth reductions of the 128-element CAA. Moreover, the numerical statistical results of the maximum SLL and mainlobe beamwidth are listed in Table 12. As can be seen, the mainlobe beamwidth obtained by the proposed IWORMLF gets narrow compare to the case of example 6, which only considers to reduce the maximum SLL. In addition, Figs. 28(a) and 28(b) show the 3D beam patterns of the uniform array and IWORMLF, respectively.

E. STABILITY TEST

Swarm intelligence optimization and evolutionary computation algorithms are usually stochastic. Therefore, the optimization results may be different in each independent run, and thus it is necessary to perform statistical tests to compare the performance of these algorithms. Therefore, there is

TABLE 12. Maximum SLLs and mainlobe beamwidth obtained by different algorithms for example 8.

	Maximum SLL (dB)	Mainlobe beamwidth (degree)
Uniform	-7.9043	4.4000
PSO	-16.4712	6.0000
BBO	-13.0202	5.6000
FA	-13.8384	5.2000
CS	-12.0047	5.2000
IWO	-17.0909	6.0000
CDA	-8.8622	4.4000
IWOA	-10.0847	5.2000
IDHS	-15.0702	5.6000
IWORMLF	-17.2685	6.0000

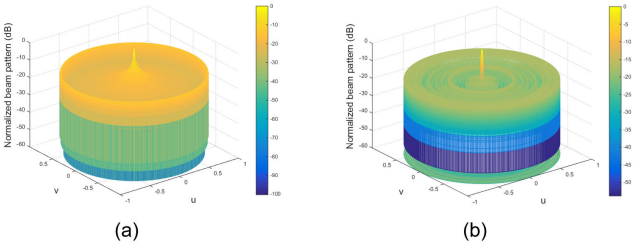

FIGURE 28. 3D beam patterns of 128-element CAA obtained by different approaches for jointly reducing the maximum SLL and mainlobe beamwidth. (a) Uniform CAA. (b) IWORMLF.

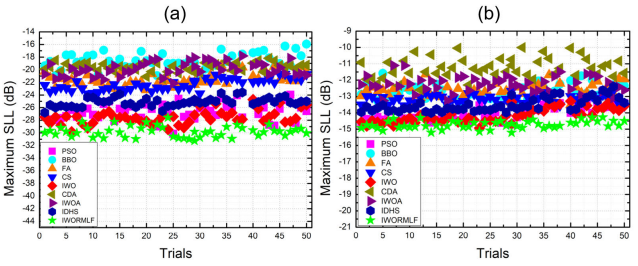

FIGURE 29. Stability tests of different algorithms for reducing the maximum SLL of 64-element antenna arrays. (a) 64-element LAA. (b) 64-element CAA.

TABLE 13. Statistical results of beam pattern optimization (64-element LAA).

	Best max SLL (dB)	Worst max SLL (dB)	Mean max SLL (dB)	SD max SLL (dB)
PSO	-29.1409	-23.9597	-26.6201	1.2750
BBO	-20.9415	-15.9344	-18.5685	1.2030
FA	-23.2175	-19.3204	-21.5364	1.0046
CS	-23.7896	-20.6507	-22.3302	0.8772
IWO	-29.8214	-24.7305	-27.5081	1.1476
CDA	-21.3989	-18.1801	-19.5901	0.6675
IWOA	-22.1546	-17.8114	-19.8971	1.0659
IDHS	-26.7775	-23.5916	-25.1228	0.6867
IWORMLF	-31.2439	-27.5844	-29.8123	0.8399

TABLE 14. Statistical results of beam pattern optimization (64-element CAA).

	Best max SLL (dB)	Worst max SLL (dB)	Mean max SLL (dB)	SD max SLL (dB)
PSO	-14.7210	-13.3030	-14.0422	0.4150
BBO	-13.9015	-11.5890	-12.7623	0.4734
FA	-13.5183	-11.6392	-12.6485	0.4291
CS	-13.5706	-12.6102	-13.1455	0.2380
IWO	-14.9317	-13.2859	-14.1896	0.4292
CDA	-12.6061	-10.0042	-11.2485	0.6160
IWOA	-13.2678	-11.1052	-12.2490	0.4748
IDHS	-14.0066	-12.3951	-13.5317	0.4074
IWORMLF	-15.2181	-14.2710	-14.7297	0.2372

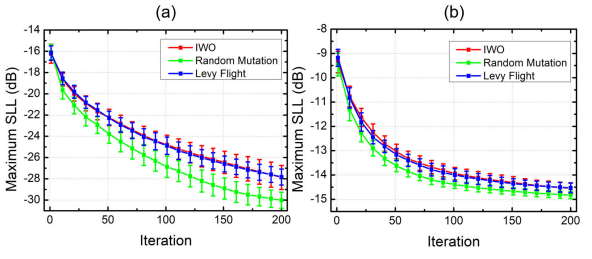

FIGURE 30. Average convergence rates of different improvement factors in the tests. (a) 64-element LAA. (b) 64-element CAA.

a need to test the stability performances of the proposed IWORMLF and other algorithms for the beam pattern optimizations. We select the 64-element LAA and CAA as the samples and the maximum SLL reductions of these two antenna arrays are considered for the tests. In this work, each test was independently run 50 times, and the results are shown in Figs. 29(a) and 29(b), respectively, for the 64-element LAA and CAA cases. Moreover, the statistical results are shown in Tables 13 and 14, respectively. The figures and tables show that the proposed IWORMLF algorithm achieves the overall best performance in terms of the stability.

F. VERIFICATION OF EFFECTIVENESS OF IMPROVED FACTORS

Test cases were designed to verify the effectiveness of the introduced random mutation operator and Lévy flight mechanism. In the tests, we compared the maximum SLLs obtained using the conventional IWO, IWO with the random mutation operator, and IWO with the Lévy flight mechanism, respectively, for the 64-element LAA and CAA conditions. These tests were also independently run 50 times for each case in order to prevent bias, and the 95% confidence interval bars are shown in Figs. 30(a) and 30(b) for LAA and CAA, respectively. As shown in the figures, IWO with the random mutation operator can effectively improve the convergence rate and the accuracy compared with the conventional IWO for the optimization of both the LAA and the CAA. Moreover, these figures also indicate that the Lévy flight mechanism improves the stability of the solution. As shown by the analysis in section 5, the random mutation operator is able to improve the population diversity, while the Lévy flight mechanism can enhance the global search ability of the algorithm. Thus, the two introduced improved factors have the ability to improve on the performance of the conventional IWO algorithm.

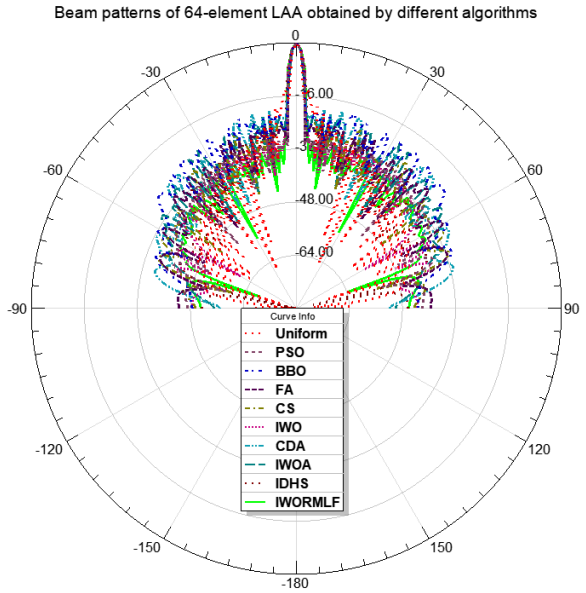

FIGURE 31. EM simulation results obtained by different algorithms for 64-element LAA.

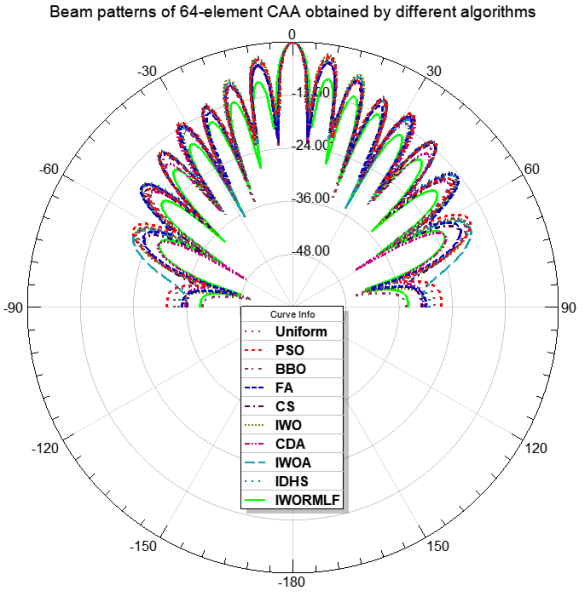

FIGURE 32. EM simulation results obtained by different algorithms for 64-element CAA.

G. EFFECT OF MUTUAL COUPLING

In this work, the mutual coupling between the elements is not considered when formulating the optimization problems. However, the mutual couping exists in practical antenna arrays [56]. Thus, it is necessary to conduct EM simulations to evaluate if the proposed algorithm is also effective for optimizing the beam patterns with the existence of mutual coupling.

First, we design a physical structure of the antenna element based on ANSYS Electromagnetics (HFSS) and adopt this element to construct 64-element LAA and CAA, respectively. Then, similar to [9], the optimized excitation currents obtained in the ideal condition that without considering the mutual coupling are plugged into HFSS, which is a more practical simulation platform, to verify that if the solutions obtained from the ideal environment are effective for the practical environment. Figs. (31) and (32) show the 2D beam pattern results obtained by different approaches of the EM simulations, and the numerical results of the maximum SLLs of these approaches are shown in Table 15. It can be seen from the figures and table that all the optimization algorithms are able to suppress the maximum SLL of the antenna array with the consideration of mutual coupling. However, the proposed IWORMLF achieves the best performance compared to other algorithms. Therefore, similar to the conclusions in Refs. [34] and [57], the beam pattern optimizations in the ideal environment may provide general overviews of the effectiveness of different methods.

TABLE 15. Numerical results obtained by different algorithms for reducing the maximum SLLs of 64-element LAA and CAA in EM simulations.

	Maximum SLL (dB) (64-element LAA)	Maximum SLL (dB) (64-element CAA)
Uniform	-13.8027	-2.1500
PSO	-27.2824	-2.7689
BBO	-19.2343	-3.3219
FA	-23.5189	-4.0143
CS	-22.1959	-4.3007
IWO	-28.1841	-2.3477
CDA	-19.0520	-4.2519
IWOA	-20.6349	-3.9643
IDHS	-24.8501	-2.8425
IWORMLF	-29.4716	-7.7329

VII. DISCUSSIONS OF THE BOUNDARY HANDLING TECHNOLOGY

In this section, the solution boundary handling technology of the algorithm is discussed.

In each iteration of the algorithm, the updated solutions may be beyond the boundary or constraints of the algorithm. Thus, the solution boundary handling technologies are necessary to adjust the values of solutions to fit the boundary of the algorithm. Moreover, the performance of the algorithm may be affected by the boundary handling technologies since these technologies are actually can be regarded as the solution update methods. As is introduced in [58], the position regulated boundary conditions (PRBCs) can achieve trade-off between global optimal solution and immature fast convergence minimum. PRBCs have several boundary algorithms including the hard position relocation, random position relocation, symmetric position relocation and hysteretic boundary conditions [58]. In this paper, we use the hard position relocation which is a simple method in the proposed IWORMLF algorithm for handling the boundary as well as the constraints. In this method, the candidate solutions will be relocated the particular fixed values within the scope of the solution space when the solutions are beyond the boundary.

However, it has been demonstrated by [59] that the hysteretic boundary handling method used in PSO algorithm may have better performance than the hard boundary method for the antenna array beam pattern synthesis problems. Therefore, we will use hysteretic boundary handing method in our future work.

VIII. CONCLUSION

This paper proposes a novel IWORMLF algorithm for the SLL reduction and the joint SLL and mainlobe beamwidth reductions of LAAs and CAAs. IWORMLF introduces two improved factors to enhance the accuracy and increase the convergence rate of the conventional IWO algorithm: the random mutation operator and the Lévy flight mechanism. This makes it more suitable for solving optimization problems. Simulations were conducted to evaluate the performance of the new proposed algorithm. The CEC 2014 function set was adopted to test the effectiveness of the proposed algorithm in the optimization of common functions. Then, the key parameter of IWORMLF was tuned such that the algorithm becomes more suitable for solving antenna array beam pattern optimization problems. The beam pattern optimization consequence indicates that the proposed algorithm achieves a better performance than several very recent algorithms and some classical evolutionary algorithms. Moreover, the stability of IWORMLF was evaluated, and the results show that the proposed algorithm has the best performance compared with other algorithms. In addition, the effectiveness of the improved factors was verified. Finally, the performance of IWORMLF for optimizing the beam patterns with considering the mutual coupling is evaluated by EM simulations. Accordingly, the proposed IWORMLF has better performances in terms of the convergence rate, accuracy, and stability for the beam pattern optimizations of LAA and CAA.

ACKNOWLEDGMENT

We would like to thank the anonymous referees for their many valuable suggestions and comments.

REFERENCES

[1] S. Liang, T. Feng, and G. Sun, "Sidelobe-level suppression for linear and circular antenna arrays via the cuckoo search–chicken swarm optimisation algorithm," *IET Microw., Antennas Propag.*, vol. 11, no. 2, pp. 209–218, Jan. 2017.

[2] N. Dib, "Design of planar concentric circular antenna arrays with reduced side lobe level using symbiotic organisms search," *Neural Comput. Appl.*, vol. 30, no. 12, pp. 3859–3868, Dec. 2018.

[3] D. Z. Zhu, P. L. Werner, and D. H. Werner, "Design and optimization of 3-D frequency-selective surfaces based on a multiobjective lazy ant colony optimization algorithm," *IEEE Trans. Antennas Propag.*, vol. 65, no. 12, pp. 7137–7149, Dec. 2017.

[4] G. Sun, Y. Liu, S. Liang, Z. Chen, A. Wang, Q. Ju, and Y. Zhang, "A sidelobe and energy optimization array node selection algorithm for collaborative beamforming in wireless sensor networks," *IEEE Access*, vol. 6, pp. 2515–2530, 2018.

[5] G. Sun, Y. Liu, A. Wang, J. Zhang, X. Zhou, and Z. Liu, "Sidelobe control by node selection algorithm based on virtual linear array for collaborative beamforming in WSNs," *Wireless Pers. Commun.*, vol. 90, no. 3, pp. 1443–1462, Oct. 2016.

[6] H. Li, Y. Liu, G. Sun, A. Wang, and S. Liang, "Beam pattern synthesis based on improved biogeography-based optimization for reducing sidelobe level," *Comput. Electr. Eng.*, vol. 60, pp. 161–174, May 2017.

[7] G. Sun, Y. Liu, J. Zhang, A. Wang, and X. Zhou, "Node selection optimization for collaborative beamforming in wireless sensor networks," *Ad Hoc Netw.*, vol. 37, pp. 389–403, Feb. 2016.

[8] G. Shen, Y. Liu, G. Sun, T. Zheng, X. Zhou, and A. Wang, "Suppressing sidelobe level of the planar antenna array in wireless power transmission," *IEEE Access*, vol. 7, pp. 6958–6970, 2019.

[9] G. Sun, Y. Liu, H. Li, J. Li, A. Wang, and Y. Zhang, "Power-pattern synthesis for energy beamforming in wireless power transmission," *Neural Comput. Appl.*, vol. 30, no. 7, pp. 2327–2342, Oct. 2018.

[10] G. Sun, Y. Liu, Z. Chen, A. Wang, Y. Zhang, D. Tian, and V. C. Leung, "Energy efficient collaborative beamforming for reducing sidelobe in wireless sensor networks," *IEEE Trans. Mobile Comput.*, to be published.

[11] A. Darvish and A. Ebrahimzadeh, "Improved fruit-fly optimization algorithm and its applications in antenna arrays synthesis," *IEEE Trans. Antennas Propag.*, vol. 66, no. 4, pp. 1756–1766, Apr. 2018.

[12] Z. Lin, M. Yao, and X. Shen, "Sidelobe reduction of the low profile multi-subarray antenna by genetic algorithm," *AEU-Int. J. Electron. Commun.*, vol. 66, no. 2, pp. 133–139, Feb. 2012.

[13] A. Recioui, "Sidelobe level reduction in linear array pattern synthesis using particle swarm optimization," *J. Optim. Theory Appl.*, vol. 153, no. 2, pp. 497–512, May 2012.

[14] O. Quevedo-Teruel and E. Rajo-Iglesias, "Ant colony optimization in thinned array synthesis with minimum sidelobe level," *IEEE Antennas Wireless Propag. Lett.*, vol. 5, pp. 349–352, 2006.

[15] C. Rocha-Alicano, D. Covarrubias-Rosales, C. Brizuela-Rodriguez, and M. Panduro-Mendoza, "Differential evolution algorithm applied to sidelobe level reduction on a planar array," *AEU-Int. J. Electron. Commun.*, vol. 61, no. 5, pp. 286–290, May 2007.

[16] S. K. Mahto, A. Choubey, and S. Suman, "Linear array synthesis with minimum side lobe level and null control using wind driven optimization," in *Proc. Int. Conf. Signal Process. Commun. Eng. Syst.*, Jan. 2015, pp. 191–195.

[17] A. Sharaqa and N. Dib, "Circular antenna array synthesis using firefly algorithm," *Int. J. RF Microw. Comput.-Aided Eng.*, vol. 24, no. 2, pp. 139–146, Mar. 2014.

[18] Y. P. Saputra, F. Oktafiani, Y. Wahyu, and A. Munir, "Side lobe suppression for X-band array antenna using Dolph-Chebyshev power distribution," in *Proc. 22nd Asia–Pacific Conf. Commun. (APCC)*, Aug. 2016, pp. 86–89.

[19] Y. Tsunoda and N. Goto, "Sidelobe suppression of planar array antennas by the multistage decision method," *IEEE Trans. Antennas Propag.*, vol. 35, no. 9, pp. 1017–1021, Sep. 1987.

[20] K. Xing, B. Liu, Z. Guo, X. Wei, R. Zhao, and Y. Ma, "Backlobe and sidelobe suppression of a Q-band patch antenna array by using substrate integrated coaxial line feeding technique," *IEEE Antennas Wireless Propag. Lett.*, vol. 16, pp. 3043–3046, 2017.

[21] Y.-B. Tian and J. Qian, "Improve the performance of a linear array by changing the spaces among array elements in terms of genetic algorithm," *IEEE Trans. Antennas Propag.*, vol. 53, no. 7, pp. 2226–2230, Jul. 2005.

[22] A. Sharaqa and N. Dib, "Design of linear and elliptical antenna arrays using biogeography based optimization," *Arabian J. Sci. Eng.*, vol. 39, no. 4, pp. 2929–2939, Apr. 2014.

[23] U. Singh and R. Salgotra, "Synthesis of linear antenna array using flower pollination algorithm," *Neural Comput. Appl.*, vol. 29, no. 2, pp. 435–445, Jan. 2018.

[24] P. Saxena and A. Kothari, "Optimal pattern synthesis of linear antenna array using grey wolf optimization algorithm," *Int. J. Antennas Propag.*, vol. 2016, pp. 1–11, 2016.

[25] L. Pappula and D. Ghosh, "Linear antenna array synthesis using cat swarm optimization," *AEU-Int. J. Electron. Commun.*, vol. 68, no. 6, pp. 540–549, Jun. 2014.

[26] A. Ahmad, A. K. Behera, S. K. Mandal, G. K. Mahanti, and R. Ghatak, "Artificial bee colony algorithm to reduce the side lobe level of uniformly excited linear antenna arrays through optimized element spacing," in *Proc. IEEE Conf. Inf. Commun. Technol.*, Apr. 2013, pp 1029-1032.

[27] P. Saxena and A. Kothari, "Ant Lion Optimization algorithm to control side lobe level and null depths in linear antenna arrays," *AEU-Int. J. Electron. Commun.*, vol. 70, no. 9, pp. 1339–1349, Sep. 2016.

[28] A. Boldini, C. A. Gonano, F. Grimaccia, M. Mussetta, A. Niccolai, R. Sgambati, and R. E. Zich, "Planar array optimization by means of SNO and StudGA," in *Proc. IEEE Antennas Propag. Soc. Int. Symp.*, Jul. 2014, pp. 1950–1951.

[29] M. Khodier and C. Christodoulou, "Linear array geometry synthesis with minimum sidelobe level and null control using particle swarm optimization," *IEEE Trans. Antennas Propag.*, vol. 53, no. 8, pp. 2674–2679, Aug. 2005.

[30] U. Singh, R. Salgotra, and M. Rattan, "A novel binary spider monkey optimization algorithm for thinning of concentric circular antenna arrays," *IETE J. Res.*, vol. 62, no. 6, pp. 736–744, Nov. 2016.

[31] G. Sun, Y. Liu, H. Li, S. Liang, A. Wang, and B. Li, "An antenna array sidelobe level reduction approach through invasive weed optimization," *Int. J. Antennas Propag.*, vol. 2018, pp. 1–16, 2018.

[32] S. Pal, A. Basak, S. Das, and A. Abraham, "Linear antenna array synthesis with invasive weed optimization algorithm," in *Proc. Int. Conf. Soft Comput. Pattern Recognit.*, Dec. 2009, pp. 161–166.

[33] A. Foudazi and A. Mallahzadeh, "Pattern synthesis for multi-feed reflector antennas using invasive weed optimisation," *IET Microw., Antennas Propag.*, vol. 6, no. 14, pp. 1583–1589, Nov. 2012.

[34] G. Sun, Y. Liu, Z. Chen, S. Liang, A. Wang, and Y. Zhang, "Radiation beam pattern synthesis of concentric circular antenna arrays using hybrid approach based on cuckoo search," *IEEE Trans. Antennas Propag.*, vol. 66, no. 9, pp. 4563–4576, Sep. 2018.

[35] M. Tubishat, M. A. M. Abushariah, N. Idris, and I. Aljarah, "Improved whale optimization algorithm for feature selection in Arabic sentiment analysis," *Appl. Intell.*, vol. 49, no. 5, pp. 1688–1707, May 2019.

[36] A. Adeli and A. Broumandnia, "Image steganalysis using improved particle swarm optimization based feature selection," *Appl. Intell.*, vol. 48, no. 6, pp. 1609–1622, Jun. 2018.

[37] L. Wang, H. Hu, R. Liu, and X. Zhou, "An improved differential harmony search algorithm for function optimization problems," *Soft Comput.*, vol. 23, no. 13, pp. 4827–4852, Jul. 2019.

[38] M. Gao, J. Shen, and J. Jiang, "Visual tracking using improved flower pollination algorithm," *Optik*, vol. 156, pp. 522–529, Mar. 2018.

[39] G. I. Sayed, A. Tharwat, and A. E. Hassanien, "Chaotic dragonfly algorithm: An improved metaheuristic algorithm for feature selection," *Appl. Intell.*, vol. 49, no. 1, pp. 188–205, Jan. 2019.

[40] U. Singh and R. Salgotra, "Synthesis of linear antenna arrays using enhanced firefly algorithm," *Arabian J. Sci. Eng.*, vol. 44, no. 3, pp. 1961–1976, Mar. 2019.

[41] G. Sun, Y. Liu, J. Li, Y. Zhang, and A. Wang, "Sidelobe reduction of large scale antenna array for 5g beamforming via hierarchical cuckoo search," *Electron. Lett.*, vol. 53, no. 16, pp. 1158–1160, 2017.

[42] A. A. Noaman, A. K. S. Abdallah, and R. S. Ali, "Optimal sidelobes reduction and synthesis of circular array antennas using hybrid adaptive genetic algorithms," in *Proc. 18th Int. Conf. Microw., Radar Wireless Commun.*, Jun. 2010, pp. 1–4.

[43] S. Jayaprakasam, S. Rahim, and C. Y. Leow, "PSOGSA-Explore: A new hybrid metaheuristic approach for beampattern optimization in collaborative beamforming," *Appl. Soft Comput.*, vol. 30, pp. 229–237, May 2015.

[44] G. G. Roy, S. Das, P. Chakraborty, and P. N. Suganthan, "Design of non-uniform circular antenna arrays using a modified invasive weed optimization algorithm," *IEEE Trans. Antennas Propag.*, vol. 59, no. 1, pp. 110–118, Jan. 2011.

[45] Z. Zhang, X. Liu, B. Zhang, and H. Li, "Pattern synthesis of time-modulated array antenna based on an improved invasive weed optimization method," *Int. J. Antennas Propag.*, vol. 2019, pp. 1–8, May 2019.

[46] Y. Liu, Y.-C. Jiao, Y.-M. Zhang, and Y.-Y. Tan, "Synthesis of phase-only reconfigurable linear arrays using multiobjective invasive weed optimization based on decomposition," *Int. J. Antennas Propag.*, vol. 2014, Oct. 2014, Art. no. 630529.

[47] R. Majumdar, A. Ghosh, S. Raha, K. Laha, and S. Das, "A quantized invasive weed optimization based antenna array synthesis with digital phase control," in *Swarm, Evolutionary, and Memetic Computing* (Lecture Notes in Computer Science), vol. 7076, B. K. Panigrahi, P. N. Suganthan, S. Das, and S. C. Satapathy, Eds. Berlin, Germany: Springer-Verlag, Dec. 2011, pp. 102–109.

[48] G. Sun, Y. Liu, S. Liang, A. Wang, and Y. Zhang, "Beam pattern design of circular antenna array via efficient biogeography-based optimization," *AEU-Int. J. Electron. Commun.*, vol. 79, pp. 275–285, Sep. 2017.

[49] A. Mehrabian and C. Lucas, "A novel numerical optimization algorithm inspired from weed colonization," *Ecol. Informat.*, vol. 1, no. 4, pp. 355–366, Dec. 2006.

[50] J. Liang, B. Y. Qu, and P. Suganthan, "Problem definitions and evaluation criteria for the CEC 2014 special session and competition on single objective real-parameter numerical optimization," Comput. Intell. Lab., Nanyang Technol. Univ., Singapore, Zhengzhou China Tech. Rep., 2013.

[51] J. Kennedy and R. Eberhart, "Particle swarm optimization," in *Proc. Int. Conf. Neural Netw.*, Nov. 2002, pp. 1942–1948.

[52] D. Simon, "Biogeography-based optimization," *IEEE Trans. Evol. Comput.*, vol. 12, no. 6, pp. 702–713, Dec. 2008.

[53] U. Singh, D. Singh, and C. Kaur, "Thinning of planar circular array antennas using firefly algorithm," in *Proc. Recent Adv. Eng. Comput. Sci.*, Mar. 2014, pp. 1–5.

[54] X.-S. Yang and S. Deb, "Cuckoo search via Lévy flights," in *Proc. World Congr. Nature Biol. Inspired Comput.*, Dec. 2009, pp. 210–214.

[55] S. Das, G. R. Hardel, P. Chakravorty, D. Mandal, R. Kar, and D. S. P. Ghoshal, "Optimization of antenna arrays for SLL reduction towards Pareto objectivity using GA variants," in *Proc. IEEE Symp. Comput. Intell.*, Dec. 2015, pp. 1164–1169.

[56] P. Chakravorty and D. Mandal, "Radiation pattern correction in mutually coupled antenna arrays using parametric assimilation technique," *IEEE Trans. Antennas Propag.*, vol. 64, no. 9, pp. 4092–4095, Sep. 2016.

[57] S. Jayaprakasam, S. K. Abdul Rahim, C. Y. Leow, T. O. Ting, and A. A. Eteng, "Multiobjective beampattern optimization in collaborative beamforming via NSGA-II with selective distance," *IEEE Trans. Antennas Propag.*, vol. 65, no. 5, pp. 2348–2357, May 2017.

[58] P. Chakravorty and D. Mandal, "Role of boundary dynamics in improving efficiency of particle swarm optimization on antenna problems," in *Proc. IEEE Symp. Comput. Intell.*, Dec. 2015, pp. 1157–1163.

[59] P. Chakravorty and D. Mandal, "Hysteretic boundary conditions for PSO of antenna array pattern synthesis," *Procedia Comput. Sci.*, vol. 45, pp. 628–634, 2015. [Online]. Available: http://www.sciencedirect.com/science/article/pii/S1877050915003543

TINGTING ZHENG received the B.S. degree in software engineering from Jilin University, China, in 2017, where she is currently pursuing the Ph.D. degree in computer science. Her research interests include wireless communications and optimization.

YANHENG LIU received the M.Sc. and Ph.D. degrees in computer science from Jilin University, China, where he is currently a Professor. His primary research interests include network security, network management, mobile computing network theory, and applications.

GENG SUN (Member, IEEE) received the B.S. degree in communication engineering from Dalian Polytechnic University, in 2007, and the Ph.D. degree in computer science and technology from Jilin University, in 2018. He was a Visiting Researcher with the School of Electrical and Computer Engineering, Georgia Institute of Technology, GA, USA. He currently holds a postdoctoral position with Jilin University. His research interests include wireless sensor networks, antenna arrays, collaborative beamforming, and optimization.

LIN ZHANG received the bachelor's degree in electrical engineering and automation from the Changchun University of Technology and the master's degree in computer science and technology from Jilin University, in 2013 and 2016, respectively. He is currently an Assistant Engineer with the Financial Department of Jilin University. His research interests include wireless sensor networks.

SHUANG LIANG received the M.S. degree in software engineering from Jilin University, China, in 2016, where she is currently pursuing the Ph.D. degree in computer science. Her research interests focus on wireless communication and the design of array antennas.

AIMIN WANG received the B.S. degree in computer software and the M.S. degree in computer application technology from Jilin University, and the Ph.D. degree in communication and information systems from Jilin University. He is currently an Associate Professor with Jilin University. His research interests are wireless sensor networks and QoS for multimedia transmission.

XU ZHOU received the M.S. and Ph.D. degrees from Northeast Normal University and Jilin University, China, in 2013 and 2016, respectively. She is currently a Postdoctoral Researcher with Jilin University. Her research interests include intelligent algorithms, data mining, and complex network analysis.